Antigenic strain diversity predicts different biogeographic patterns of invasion and maintenance of anti-malarial drug resistance

Qixin He[1†*], **John K. Chaillet**[1†], **Frédéric Labbé**[2§]

[1]Department of Biological Sciences, Purdue University, West Lafayette, IN, USA;
[2]Department of Ecology and Evolution, University of Chicago, Chicago, IL, USA

***For correspondence:** heqixin@purdue.edu (QH)

[†]These authors contributed equally to this work

Present address: [§]CIRAD, UMR PVBMT, F-97410 Saint Pierre, La Réunion, France

Abstract The establishment and spread of anti-malarial drug resistance vary drastically across different biogeographic regions. Though most infections occur in Sub-Saharan Africa, resistant strains often emerge in low-transmission regions. Existing models on resistance evolution lack consensus on the relationship between transmission intensity and drug resistance, possibly due to overlooking the feedback between antigenic diversity, host immunity, and selection for resistance. To address this, we developed a novel compartmental model that tracks sensitive and resistant parasite strains, as well as the host dynamics of generalized and antigen-specific immunity. Our results show a negative correlation between parasite prevalence and resistance frequency, regardless of resistance cost or efficacy. Validation using chloroquine-resistant marker data supports this trend. Post discontinuation of drugs, resistance remains high in low-diversity, low-transmission regions, while it steadily decreases in high-diversity, high-transmission regions. Our study underscores the critical role of malaria strain diversity in the biogeographic patterns of resistance evolution.

Introduction

Prolonged usage of antimicrobial drugs almost always results in the emergence and spread of resistant strains (***zur Wiesch et al., 2011***). The history of falciparum malaria chemotherapy over the last hundred years witnessed a succession of the spread of resistance to five classes of drugs region by region (***Blasco et al., 2017***). However, the patterns of drug resistance evolution, such as the speed of establishment and equilibrium frequencies, differ drastically across different biogeographic regions. Even though *de novo* resistant alleles are constantly generated, widespread resistant strains can almost always be traced back to two unstable transmission regions, i.e., Southeast Asia (especially the Greater Mekong Subregion) and South America (***Ecker et al., 2012***; ***Dondorp et al., 2009***; ***Noedl et al., 2008***). While the frequencies of resistant genotypes often sweep close to fixation in these regions under persistent drug usage (***Chaijaroenkul et al., 2011***; ***Best Plummer et al., 2004***), their frequencies are more variable in endemic transmission regions such as sub-Saharan Africa (***Talisuna et al., 2002***). More interestingly, while in high-transmission regions, a steady decrease of resistant genotypes often ensues from reducing the particular drug usage (***Narh et al., 2020***; ***Hemming-Schroeder et al., 2018***), resistant genotypes are maintained at high frequency in low or unstable transmission regions even after the abandonment of the drug for several decades (***Lanteri et al., 2014***).

Plenty of mathematical models have been developed to explain some, but not all of the empirical drug-resistance patterns. Various relationships between transmission intensity and stable frequencies of resistance were discovered, each of which has some empirical support: 1) transmission intensity does not influence the fate of resistant genotypes (Model: ***Koella and Antia*** (***2003***); In a recent stochastic model (***Masserey et al., 2022***), access to treatment in symptomatic cases was the dominant factor that determines selection for resistance; Empirical: ***Diallo et al.*** (***2007***); ***Shah et al.*** (***2011***, 2015); 2) resistance increases in frequency and slowly decreases with increasing transmission rates (Models: ***Klein et al.*** (***2008***, 2012)); and 3) Valley phenomenon: resistance can be fixed at both high and low end of transmission intensity (Model: ***Artzy-Randrup et al.*** (***2010***); Empirical: ***Talisuna et al.*** (***2002***)). Other stochastic models predict that it is harder for resistance to spread in high transmission regions, but patterns are not systematically inspected across the parameter ranges (Model: ***Whitlock et al.*** (***2021***); Model and examples in ***Ariey and Robert*** (***2003***)); Under non-equilibrium scenarios, i.e., where insecticides or bednets temporarily reduced transmission, reductions in resistance frequency were also observed (***Alifrangis et al., 2003***; ***Mharakurwa et al., 2004***; ***Myers-Hansen et al., 2020***). Differences in these model predictions can be attributed to three types of model assumptions: 1) whether and how population immunity is considered, 2) how the cost of resistance is modeled, and 3) whether and how multiplicity of infection (MOI) is included. Although the great advances in malaria agent-based models (ABMs) enabled the inclusion of more detailed biological processes (***Maire et al., 2006***; ***Masserey et al., 2022***; ***He et al., 2021***; ***Labbé et al., 2023***), the complexity of ABMs limits a direct application to analytical investigation. It is, therefore, critical to formulate a generalizable mathematical model that captures the most important biological processes that directly impact the survival and transmission of the parasites.

While most models have explored factors such as drug usage (***Koella and Antia, 2003***; ***Klein et al., 2012***), treatment rate (***Masserey et al., 2022***), vectorial capacity (***Artzy-Randrup et al., 2010***; ***Bushman et al., 2018***), within-host competition (***Bushman et al., 2018***; ***Hastings, 2006***), population immunity (***Klein et al., 2008***; ***Artzy-Randrup et al., 2010***), and recombination (***Curtis and Otoo, 1986***; ***Dye and Williams, 1997***; ***Hastings, 1997***; ***Hastings and D'Alessandro, 2000***), strain diversity of parasites has not been explicitly considered in mathematical models of drug resistance. Yet, orders of magnitude differentiate antigenic diversity of *Plasmodium faciparum* strains among biogeographic zones and drive key differences in epidemiological features (***Chen et al., 2011***; ***Tonkin-Hill et al., 2018***). Hyper-diverse antigens of parasites in sub-Saharan Africa emerged from the long-term coevolutionary arms race among hosts, vectors, and parasites (***Volkman et al., 2001***). In endemic regions of falciparum malaria, hosts do not develop sterile immunity and can constantly get reinfected with reduced symptoms (***Day and Marsh, 1991***). These asymptomatic carriers of the parasite still constitute part of the transmission and serve as a reservoir of strain diversity (***Tiedje et al., 2017***; ***Bonnet et al., 2003***) despite the fact that parasite prevalence decreases with host age in endemic regions (***Aron, 1983***). This age-prevalence pattern was attributed to acquired immunity after repeated infections and represented as different generalized immunity classes in disease dynamics models (***Dietz et al., 1974***; ***Molineaux et al., 1980***; ***Klein et al., 2008***). Later advances in molecular epidemiology indicate the importance of strain-specific immunity (***Bull et al., 1999***).

During the asexual blood stage, intra-erythrocytic parasites express adhesin proteins at the red blood cell surface that help mediate binding to the epithelial layers of vasculature to avoid the clearance by spleen during circulation (***Bull et al., 1998***). One of the major surface proteins, *P. falciparum* erythrocyte membrane protein 1 (*Pf*EMP1), is encoded by *var* genes, a gene family of 60 different copies within a single parasite genome (***Rask et al., 2010***). Immune selection maintains the composition of *var* genes between different strains with minimal overlap (***He et al., 2018***). In high endemic regions, many antigenically distinct strains (or modules of strains) coexist in the transmission dynamics (***Pilosof et al., 2019***). Whether the hosts have seen the specific variants of the *var* genes largely determines the clearance rate of the parasites (***Barry et al., 2011***; ***Djimdé et al., 2003***). Therefore, it is reasonable to suspect that variation in host-specific immunity, acquired from exposure to local antigenic diversity, plays a key role in local transmission dynamics as well as

the fate of resistance. Thus, under the same vectorial capacity, different strain diversity results in significant changes in population-level immunity and transmission intensity, and the ensuing epidemiological patterns, such as multiplicity of infection (MOI), age-prevalence curve, and the ratio of asymptomatic infections (***Tiedje et al., 2017***; ***Ruybal-Pesántez et al., 2022***). These changes, in turn, alter the fate of resistance invasion. Therefore, in addition to generalized immunity represented in earlier studies, models need to formally incorporate specific immunity.

Another challenging aspect for earlier models is whether and how multiclonal infections (those with MOI> 1) are considered. Due to malaria's long duration of infection (***Collins and Jeffery, 1999***), it is common for the host to carry infections that are contracted from separate bites, referred to as superinfections. Meanwhile, hosts can also receive multiple genetically distinct strains from a single bite, especially in high-transmission endemic regions (***Nkhoma et al., 2018***; ***Wong et al., 2017***; ***Henden et al., 2018***). Susceptible-Infected-Recovered (SIR) Models that only consider non-overlapping infections (***Koella and Antia, 2003***; ***Klein et al., 2008***; ***Artzy-Randrup et al., 2010***) cannot incorporate within-host dynamics of strains explicitly, which strongly impacts the fitness of resistant genotypes (***de Roode et al., 2004***; ***Bushman et al., 2016***). Other superinfection models employ complex structures or specific assumptions that make it hard to link MOI with strain diversity or host immunity (***Koella and Antia, 2003***; ***Klein et al., 2012***).

Here we present a novel ordinary differential equations (ODE) model that represents how strain diversity and vectorial capacity influence transmission intensity, hosts' strain-specific and generalized immunity, and the resulting MOI distribution. In this model, strain-specific immunity toward diverse surface proteins determines the probability of new infections. In contrast, generalized immunity of the hosts determines the likelihood of clinical symptoms. Hosts are less likely to show symptoms with repeated infections but can still be re-infected by antigenically new strains and contribute to transmission. Our modeling strategy combines the advantages of both the traditional compartmental epidemiological models (i.e., tracking transmission dynamics and population immunity responses to different levels of transmission intensity) (***Koella and Antia, 2003***; ***Klein et al., 2008***; ***Artzy-Randrup et al., 2010***; ***Klein et al., 2012***) and population genetics ones (i.e., tracking within-host dynamics with detailed consideration of fitness cost and competition among strains) (***Curtis and Otoo, 1986***; ***Dye and Williams, 1997***; ***Hastings, 2006***, ***1997***; ***Hastings et al., 2002***). With varying strain diversity, vectorial capacity, resistance cost, and symptomatic treatment rates, we explore the key questions outlined above: whether strain diversity modulates the equilibrium resistance frequency given different transmission intensities, as well as changes in this frequency after drug withdraw, and whether the model explains the biogeographic patterns of drug resistance evolution. We then verify the main qualitative outcome from the model against the empirical biogeographic patterns of chloroquine resistance evolution.

Results

Model structure

In the compartmental ODE model, hosts' strain-specific immunity (S) regulates infectivity of parasite strains, while generalized immunity (G) determines symptomatic rate (***Figure 1***; see model details in Material and Methods and ***Appendix 1***). Hosts are tracked in different classes of generalized immunity (G) and drug usage status (untreated, U; treated, D). Hosts move to a higher G class if they have cleared enough infections and go back to a lower class if they lose generalized immunity (***Figure 1***B: $G_i \rightarrow G_j$, ***Figure 1—figure Supplement 1***). Lower G classes correspond to more severe and apparent symptoms, which increase the likelihood of being treated by drugs ($U \rightarrow D$), as evidenced from most impacted countries where children are the main symptomatic hosts (***Tiedje et al., 2017***). The population sizes of resistant (PR) or sensitive (wild-type; PW) parasites are tracked separately in host compartments of different G and drug status. Since hosts can harbor multiple parasite strains, parasites are assumed to be distributed independently and randomly among hosts within the same compartment (***Anderson and May, 1978***). Parasites can

move between the compartments via the movement of hosts that harbor them, or can be added to or subtracted from the compartments via new infections and parasite clearance respectively. PW can be cleared by host immunity and drug-treatment, while PR can only be cleared by host immunity. However, PR has a cost, s, in transmissibility, and the cost is higher in mixed-genotype (s_{mixed}) infections than in single-genotype infections (s_{single}) following (***Bushman et al., 2016***; ***Harrington et al., 2009***; ***Bushman et al., 2018***).

Instead of tracking antigenic diversity explicitly, we assume parasites have $n_{strains}$ with unique antigen compositions at the population level. We incorporate specific immunity by calculating the probability of seeing a new strain given a G class upon being bitten by an infectious mosquito,

$$\eta_i = (1 - \frac{1}{n_{strains}})^{v_i} \tag{1}$$

where v_i is the average number of cumulative infections received and cleared by a host in class G_i, and is updated at each time step as determined by the immune memory submodel (see ***Appendix 1***).

Appropriate pairing of strain diversity and vectorial capacity

To avoid assuming an arbitrary level of strain diversity given transmission rate, we explored the impacts of the number of strains and vectorial capacity on prevalence separately across the empirical range observed in the field. Specifically, the number of unique strains ranges from 6 to 447, which corresponds to a pool of 360 (typical of low transmission regions) to 27,000 unique surface antigens (typical of sub-Saharan Africa) (***Chen et al., 2011***; ***Tonkin-Hill et al., 2018***). Mosquito bites follow a sinusoidal curve (***Appendix 1***), representing a peak transmission period in the wet season, and low transmission in the dry season annually, with a mean vectorial capacity from 0.007 to 5.8. This range encompasses the lowest vectorial capacity to maintain a constant transmission to the level of high transmission settings in Africa (***Garrett-Jones and Shidrawi, 1969***). We observe that the range of vectorial capacity that leads to the highest prevalence given a specific strain diversity increases from low diversity to high diversity (see grey area in ***Figure 2***A, ***Figure 2—figure Supplement 1***). This is consistent with the strain diversity being the outcome of long-term coevolution between parasite transmission and host immunity, whereby high transmission regions usually correspond to high antigenic diversity and low transmission regions exhibit low antigenic diversity (***Chen et al., 2011***; ***Tonkin-Hill et al., 2018***). Therefore, for the following analyses, we focused on the parameter combinations within the grey area in ***Figure 2***A, where diversity tracks transmission intensity.

Drug-resistance and disease prevalence

In general, the frequency of resistance decreases with increasing parasite prevalence (***Figure 2***B,C), except for very low vectorial capacity, where resistance always fixes because wild-type strains cannot sustain transmissions under treatment (***Figure 2—figure Supplement 1***, ***Figure 2—figure Supplement 3***,***Figure 2—figure Supplement 4***). The fitness costs of single- and mixed-genotype infections, symptomatic treatment rate, and the efficacy of drug resistance only influence the slope of the relationship and the range of coexistence of resistant and wild-type parasites, but do not alter the negative relationship qualitatively (***Figure 2***C; ***Figure 2—figure Supplement 3***,***Figure 2—figure Supplement 4***). Therefore, in the following sections, we only present results from one set of fitness cost combinations (i.e., $s_{single} = 0.1$ and $s_{mixed} = 0.9$ to be consistent with an earlier modeling study of parasite competition (***Bushman et al., 2018***)).

The negative relationship between resistance and prevalence is corroborated by the empirical observation of the chloroquine-resistant genotype. The global trend of the critical chloroquine-resistant mutation *pfcrt* 76T follows an overall decline in frequency with increasing prevalence, which qualitatively agrees with the similar relationship from our model (Fig ***Figure 3***; beta regression, p-value$< 2e-16$). Samples from Asia and South America cluster around low prevalence and

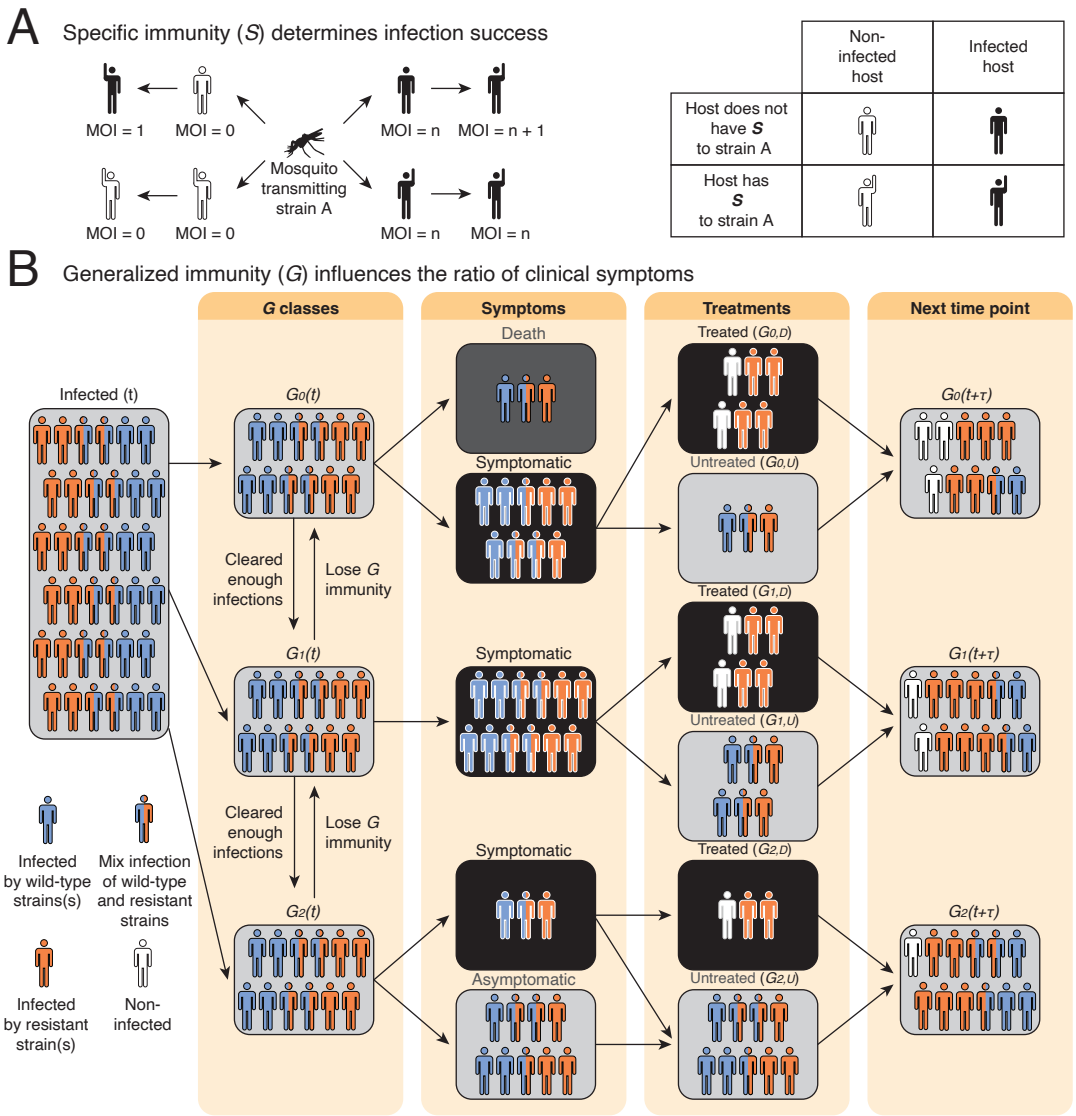

Figure 1. Schematic illustration of transmission rules and acquisition of host immunity within the compartmental ODE model (see *Figure 1—figure Supplement 1* for a detailed representation of the compartment model). **(A)** Rules for new infections given the host's past infection history and current multiplicity of infection (i.e., MOI). Upon transmission of a specific parasite strain A, if the host has had an infection of strain A in the past (hands raised), a new infection will not be added to the current MOI; instead, the infection will be considered cleared and added to the total number of cleared infections; if the host is new to strain A and does not have specific immunity to it (inferred from Eq. 1), a new infection will be added (i.e., MOI increase by 1) as long as MOI does not exceed the carrying capacity of coexisting strains. **(B)** Rules of symptomatic infections and treatment in the different generalized immunity (G) classes. With increasing generalized immunity (G), hosts are less likely to show clinical symptoms. Hosts in G_0 have a risk of death in addition to symptomatic infections; Hosts in G_1 do not die from infections but show symptoms upon new infections; Hosts in G_2 carry asymptomatic infections most of the time with a slight chance of showing symptoms. Symptomatic infections result in a daily treatment rate that removes the infections caused by wild-type strains. Hosts that have cleared enough number of infections will move to the next G class. Hosts will move back to a lower G class when the generalized immunity memory is slowly lost if not boosted by constant infections.

Figure 1—figure supplement 1. Compartment model of drug resistance evolution.

high resistance regions, whilst samples from Oceania and Africa display a wide range of prevalence and resistance frequency.

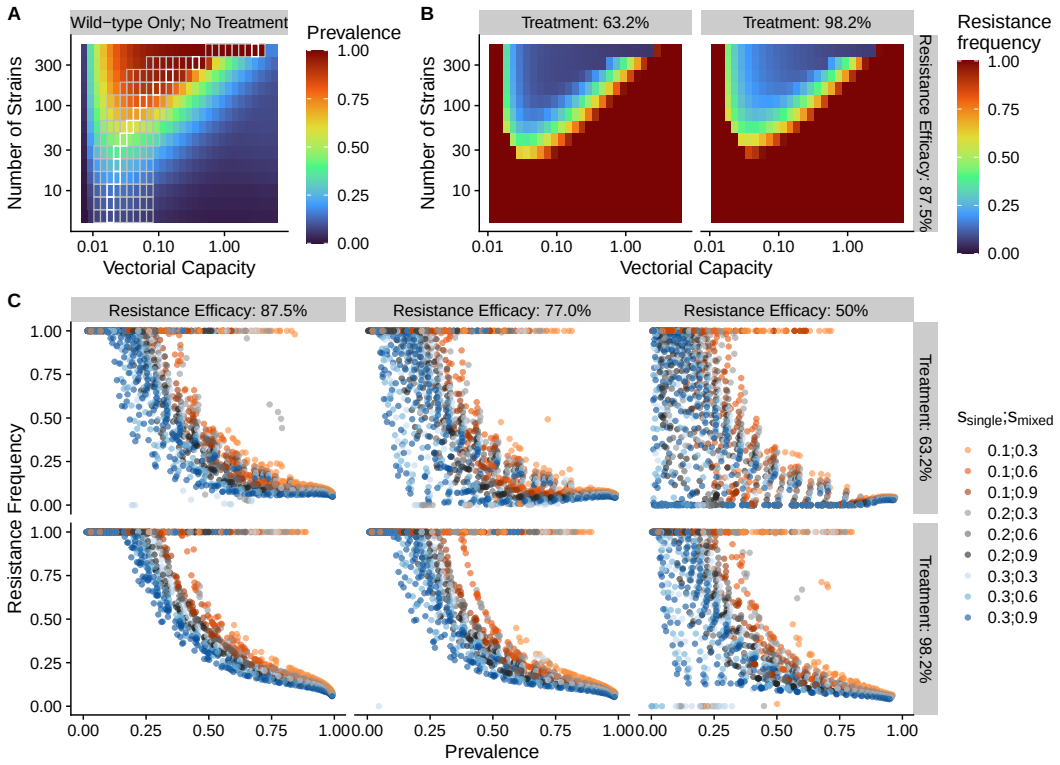

Figure 2. The frequency of resistance under varying strain diversity and vectorial capacity. (A) The heatmap shows a nonlinear parasite prevalence response given increasing vectorial capacity and the number of strains under no drug treatment, with warmer colors representing high prevalence and cooler colors representing low prevalence. X and Y axes correspond to increasing vectorial capacity and the number of strains in logarithmic scales. White tiles indicate the highest prevalence given a fixed number of strains. **(B)** The heatmaps show resistance frequencies under varying strain diversity and vectorial capacity at two levels of drug treatment rate, with warmer colors representing higher resistance frequency (in this example, s_{single} = 0.1, s_{mixed} = 0.9). **(C)** A negative relationship between parasite prevalence and resistance frequency. The color of the points indicates combinations of resistance fitness costs in hosts with resistant strains alone (s_{single}) or mixed infections of resistant and wild-type strains (s_{mixed}).

Figure 2—figure supplement 1. Prevalence given the combination of vectorial capacity and the number of strains from no treatment to high treatment rate for wild-type-only infections.

Figure 2—figure supplement 2. Infectivity of a new infection as a function of the number of strains and mean immunity.

Figure 2—figure supplement 3. Relationship between parasite prevalence and resistance frequency under full treatment.

Figure 2—figure supplement 4. Relationship between parasite prevalence and resistance frequency under partial treatment.

Dynamics of resistance invasion

The pattern of drug-resistance and disease prevalence arises from the interaction between host immunity, drug treatment, and resistance invasion. In order to inspect the dynamics of resistance invasion in detail, we select a subset of strain diversity and vectorial capacity combinations as representative scenarios for the empirical gradient of low to high transmission settings for the following analyses (white squares in ***Figure 2*** A). So far, we have assumed that strain diversity and vectorial capacity may vary independently. However, in empirical settings, strain diversity is the outcome of long-term coevolution between parasite transmission and host immunity, whereby high transmission regions usually correspond to high antigenic diversity and low transmission regions exhibit low antigenic diversity (***Chen et al., 2011***). Therefore, given the level of strain diversity, we picked

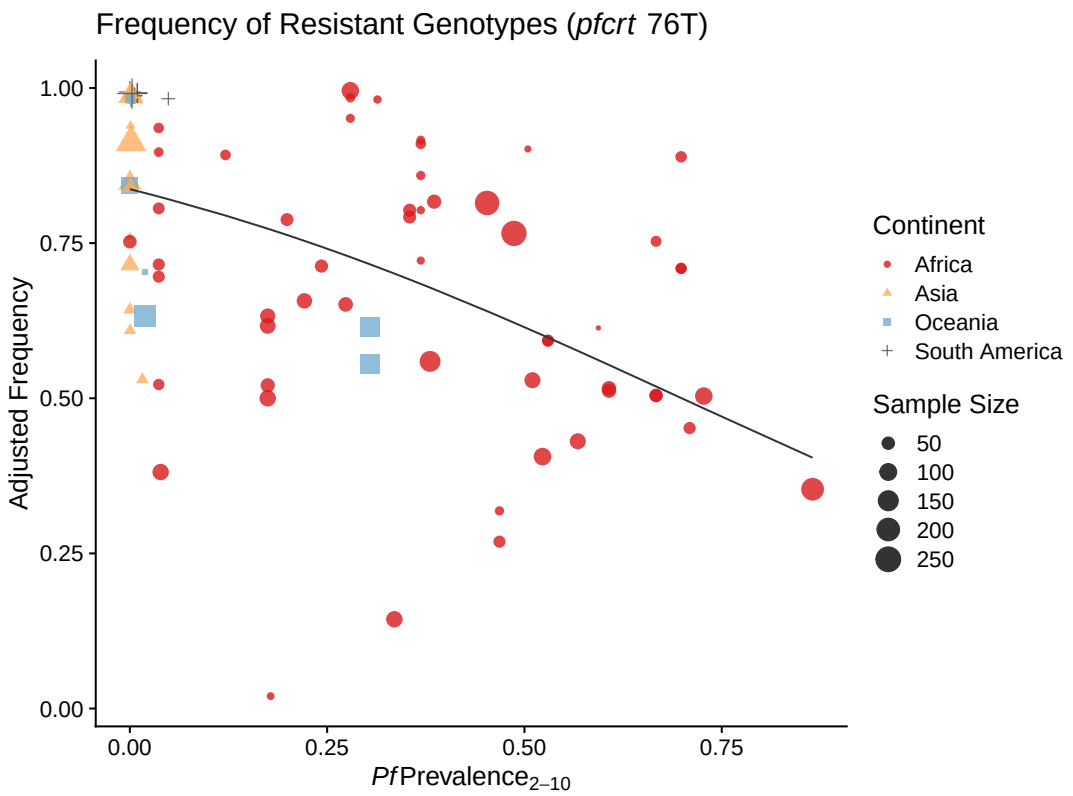

Figure 3. Global distribution of chloroquine-resistant genotype (*pfcrt* 76T) against *P. falciparum* prevalence in children between 2-10 yrs old. Sampling between 1990 and 2000 was included to ensure genotyping was performed largely before the policy switch of the first-line antimalarial drugs to ACT. Different shapes indicate samples from different continents, while shape sizes correspond to sample sizes for genotyping (see Methods for details).

the vectorial capacity that generates the highest prevalence. Under this constraint, the relationship between vectorial capacity and prevalence or diversity and prevalence is monotonic, in accordance with the prevailing expectation (***Figure 4***A). From low to high diversity/transmission, hosts' generalized immunity increases accordingly (higher fraction of hosts in G_1 or G_2 classes in ***Figure 4***). When drug treatments are applied in a wild-type only transmission setting, parasite prevalence is significantly reduced (***Figure 2—figure Supplement 1***), as is host generalized immunity (***Figure 4***A upper panel). A much larger proportion of hosts stay in G_0 and G_1 when effective drug treatment is applied compared to when there is no treatment. In addition, the proportion of hosts in drug-treated status increases under higher diversity. If instead, the resistant genotype is present in the parasite population and starts invading when the drug is applied, hosts' generalized immunity is comparable at equilibrium to that of the no-treatment scenario (***Figure 4*** lower panel). The drug-treated hosts in G_0 and G_1 are comparable from low to high transmission, while the frequency of resistance decreases with increasing diversity (***Figure 4*** lower panel).

Temporal trajectories of resistance invasion show that parasite population size surges as resistant parasites quickly multiply (Fig. ***Figure 5***). In the meantime, resistance invasion boosts host immunity to a similar level before drug treatment (Fig. ***Figure 5*** upper panel). The surge in host immunity, in turn, reduces the advantage of resistant parasites, leading to a quick drop in parasite prevalence. Under a low diversity scenario, wild-type parasites quickly go extinct (Fig. ***Figure 5***A). Under high diversity, however, a high proportion of hosts in the largely asymptomatic G_2 creates a niche for wild-type parasites, because the higher transmissibility of wild-type parasites compensates for their high clearance rate under drug treatment (Fig. ***Figure 5***B). To summarize, the coex-

istence between wild-type and resistant genotypes in high diversity/transmission regions reflects an interplay between the self-limiting resistant invasion and higher transmissibility of wild-type parasites as resistant invasion elevates the overall host immunity and thus the presence of a large fraction of hosts carrying asymptomatic infections.

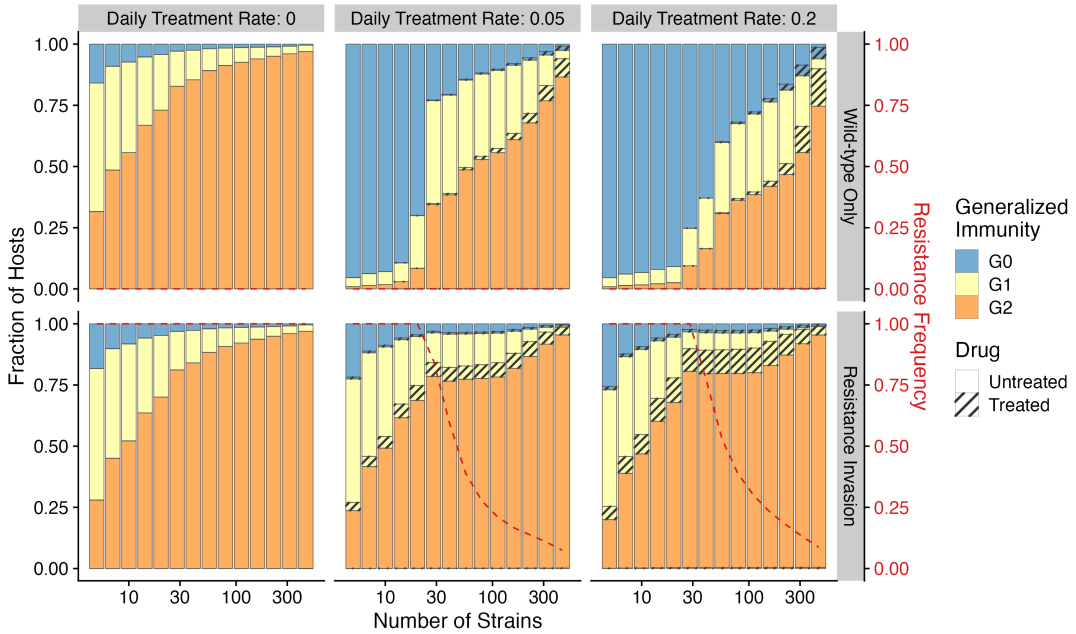

Figure 4. Relationship between host immunity, drug treatment, and resistance evolution. Fraction of hosts in different G classes with increasing strain diversity and the corresponding vectorial capacity indicated by white circles in ***Figure 1***A at equilibrium or year 50 after the invasion of resistant genotypes. Hosts in drug-treated classes are indicated by stripes. Red dotted lines show the corresponding frequency of resistance. The upper panel is generated under wild-type-only infections with increasing treatment rates. The lower panel represents resistance-only infections without treatment or resistant invasion under treatments.

Response to drug policy change

In our model, low diversity scenarios suffer the slowest decline in resistant genotypes after switching to different drugs. In contrast, resistance frequency plunges quickly in high-diversity regions when the drug policy change. (***Figure 6***; ***Figure 6—figure Supplement 1***). This pattern corroborates similar observations across different biogeographic areas: while the transition of the first-line drug to ACT in Africa, such as Ghana and Kenya, resulted in a fast reduction in resistant genotypes, the reduction was only minor in Oceania, and resistant genotypes are still maintained at almost fixation in Southeast Asia and South America despite the change in the first-line drugs occurring more than 30 years ago (***Figure 7***).

Comparison to a generalized-immunity-only model

Previous results demonstrate how transmission and antigenic diversity influence host immunity and hence the infectivity and symptomatic ratio, which determine the invasion success and maintenance of resistant genotypes. In order to confirm whether antigenic diversity is required to generate these patterns, we investigated a generalized-immunity-only model, in which infectivity of a new infection per G class is set at a fixed value (i.e., taken as the mean value per G class from the full model across different scenarios; see Material and Methods). We observe a valley phenomenon (i.e., resistance frequency is both high at the two ends of prevalence; ***Figure 8***), which is qualitatively similar to ***Artzy-Randrup et al.*** (***2010***). When we compare how the host and parasite fraction in G classes change with increasing vectorial capacity, we find that because the infectivity of bites does

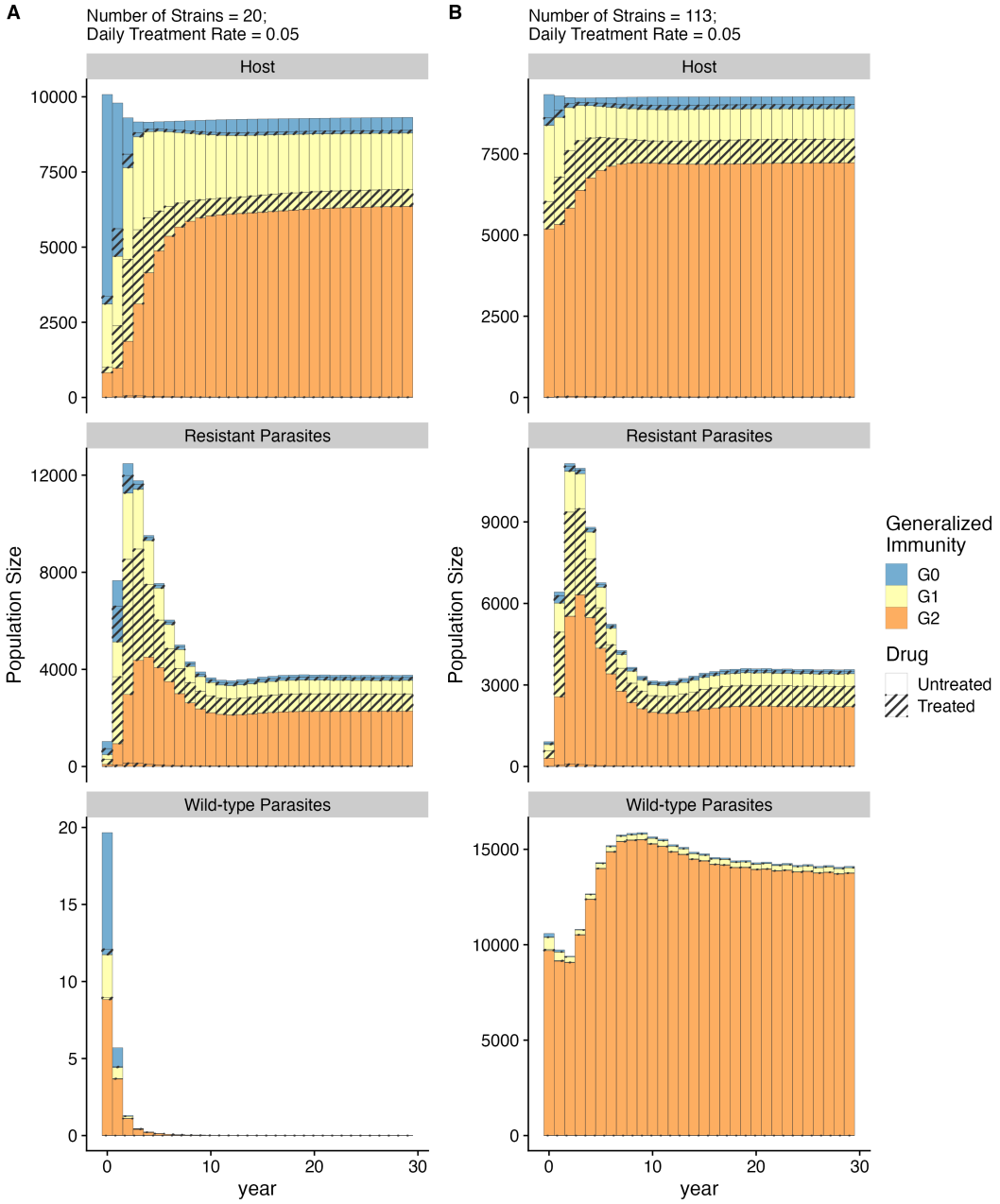

Figure 5. Temporal trajectories of resistance invasion. Host and parasite dynamics under resistance invasion are shown for lower ($n_{strains}$ = 20) **A** and higher ($n_{strains}$ = 113) diversity **B**. Because drug treatment does not affect resistant parasites, they surge quickly after introduction, thus leading to more infections. Hosts recovered from a large number of new infections move into higher G classes (from year 1-8). The high host immune protection selects against resistant parasites (year 4-10). Under low diversity, wild-type parasites quickly go to extinction **A**. Under high diversity, the less symptomatic G_2 class provides a niche for wild-type parasites to multiply (year 4-10), where the two genotypes co-exist. Meanwhile, resistant parasites dominate in hosts that are in G_0 and G_1 **B**.

not decrease as transmission increases, the number of drug-treated hosts keeps increasing in the $G2$ class, resulting in the rising advantage of resistant genotypes (***Figure 8—figure Supplement 1***). The comparison between the full model versus the generalized-immunity-only model emphasizes the importance of incorporating antigenic diversity to generate a negative relationship between resistance and prevalence.

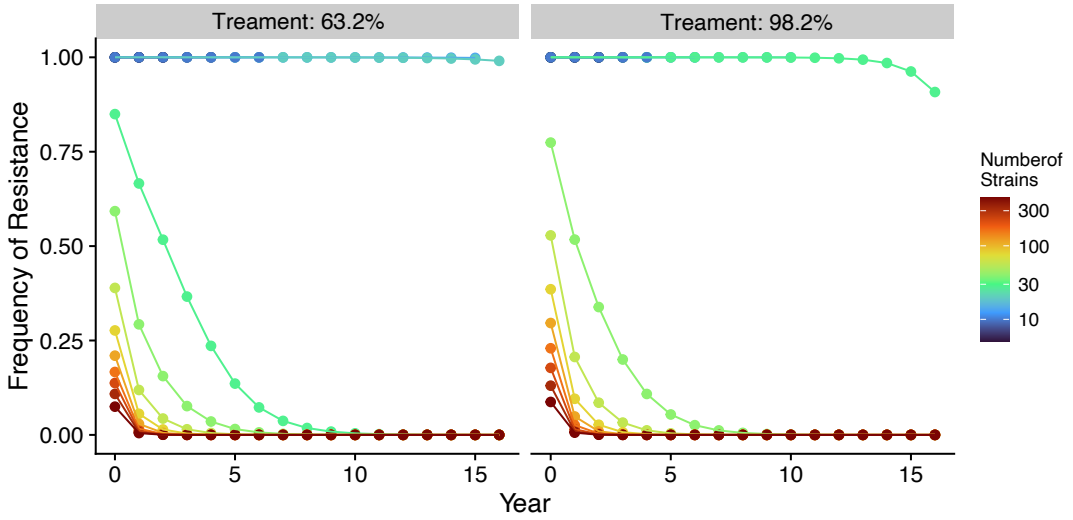

Figure 6. Changes in frequency of resistance after the first-line drug is changed. Each trajectory represents the combination of variables indicated by the white circles in ***Figure 1***A. Color from cool to warm represents increasing diversity in strains. Here the usage of the drug, to which parasites have developed resistance, is reduced to 0.52, 0.52, 0.52, 0.52, 0.21, 0.21, 0.21, 0.21, 0, 0, 0, 0, 0, 0, 0, 0 each year following the change in the treatment regime. The trajectory of reduction in resistant drug usage follows the usage survey in Western Kenya from 2003 to 2018 (***Hemming-Schroeder et al., 2018***).

Figure 6—figure supplement 1. Percentage of reduction in resistance after one year.

Discussion

In this paper, we present a theoretical argument, built on the basis of a mechanistic model, as to why different biogeographic regions show variation in the invasion and maintenance of anti-malarial drug resistance. While past models have examined the frequency of drug resistance as a consequence of transmission intensity and generalized immunity, these models, unlike ours, failed to reproduce the observed patterns of monotonic decreasing trend of resistance frequency with prevalence despite varying resistance costs, access to treatments or resistance efficacy. This contrast stems from two main innovations of our model. First, its formulation directly links selection pressure from drug usage with local transmission dynamics through the interaction between strain-specific immunity, generalized immunity, and host immune response. Second, this formulation relies on a macroparasitic modeling structure suitable for diseases with high variation in co-occurring infections and strain diversities (***Anderson and May, 1978***). Hosts are not tracked as infected or susceptible; rather, the distribution of infections in hosts of different immunity classes is followed so that within-host dynamics of parasites can be easily incorporated.

In essence, the dynamics of resistant genotypes of a single locus are governed by two opposing forces: the selective advantage from drug usage and the cost of resistance. Both forces emerge however from local transmission dynamics, contrary to many earlier population genetics or epidemiological models that set these as fixed parameters. For example, when a fixed fraction of hosts is assumed to be drug-treated upon infection (e.g., in ***Curtis and Otoo*** (***1986***); ***Dye and Williams*** (***1997***); ***Hastings*** (***1997***); ***Koella and Antia*** (***2003***)), the frequency of resistance is found to be unrelated to transmission intensity or requires other mechanisms to explain why resistance is prevalent in low transmission regions. Later models recognize the importance of clinical immunity gained through repeated reinfections (analogous to the $G2$ class in our model) in reducing drug usage (***Klein et al., 2008***; ***Artzy-Randrup et al., 2010***). Countries with different access to treatment (i.e., different treatment rates of symptomatic patients) also influence the net advantage of resistance (***Masserey et al., 2022***). However, in these models, the infectivity of new bites constrained by antigen diversity is not considered such that under high transmission, the clinically immune

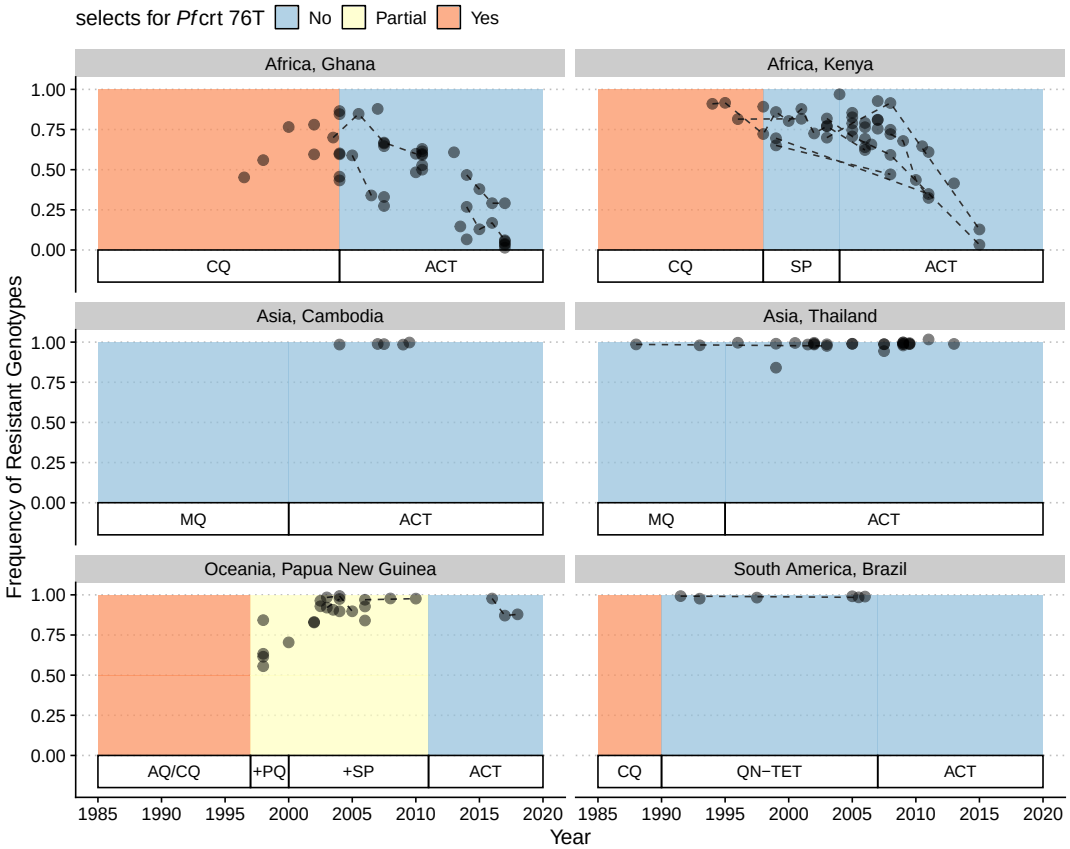

Figure 7. Changes in frequency of resistant genotypes across different biogeographic regions. Each circle represents one studied sample (at least 20 infected hosts) from one geographic location. Circles connected by dotted lines represent longitudinal samples from the same study. After the policy switch in first-line antimalarial drugs, frequencies of resistance decreased gradually in Africa, but maintained high in Asia, Oceania, and South America despite the policy change for more than 20 years. CQ: chloroquine; SP: sulfadoxine-pyrimethamine; MQ: mefloquine; AQ: amodiaquine; PQ: primaquine; QN-TET: quinine+tetracycline; ACT: artemisinin-based combination therapy.

class still receives numerous new infections, and the lowered symptomatic rate does not offset the amount of drug treatment due to new infections, giving rise to the increasing resistance prevalence at the high end of vectorial capacity (see ***Figure 8*** and ***Artzy-Randrup et al.*** (***2010***)). In contrast, in our model the selective pressure from drug treatment not only depends on the host ratio in the clinically immune class, but also on the infectivity of new bites regulated by specific immune memory. Therefore, when the host population suffers a high parasite prevalence, most hosts have experienced many infections and have entered the clinically immune class, where the drastically reduced infectivity coupled with the reduced symptomatic rate result in an overall reduced drug treatment per infection, mitigating the advantage of resistance.

Cost of resistance in terms of its form and strength is a complicated topic by itself. On the one hand, replication rates of resistant parasites are consistently found to be slower such that they produce less parasitemia during the infection than wild-type parasites (***Bushman et al., 2016***; ***ETHZentrum, 1994***; ***De Roode et al., 2005***). On the other hand, field studies also show that the transmissibility could be partially compensated by a higher gametocyte production (reviewed in ***Koella*** (***1998***)). Here we assume resistant parasites have lower transmissibility, but the cost differs between mixed- vs. single-genotype infections. Empirical and modeling studies (***Bushman et al., 2016***, ***2018***; ***de Roode et al., 2004***) have shown that within-host competition between resistant and wild-type infections results in a higher cost for resistant infections than in single genotype infections.

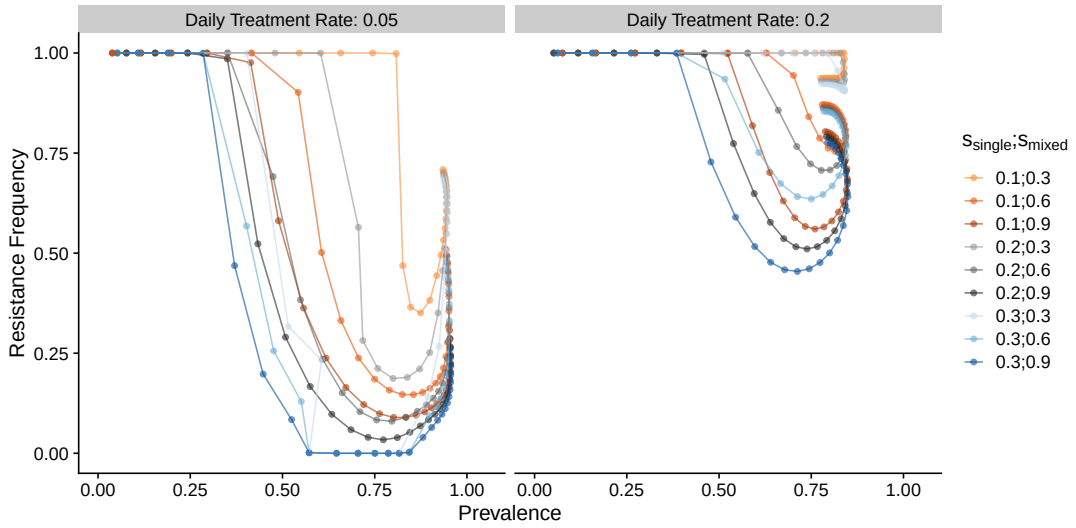

Figure 8. Relationship between parasite prevalence and resistance frequency for the generalized-immunity-only model. Paths are connected from low vectorial capacity to high vectorial capacity. Colors represent different combinations of single-genotype infection cost and mixed-genotype infection cost of resistant parasites.

Figure 8—figure supplement 1. Relationship between host immunity, drug treatment, and resistance evolution for the generalized-immunity-only model.

This phenomenon could potentially prevent resistance establishment under high-transmission settings where mixed-genotype infections are more common (***Bushman et al., 2018***). However, we did not find that the higher cost in mixed-genotype infections influenced the qualitative pattern of a negative relationship between transmission intensity (represented by parasite prevalence) and resistance frequency. In addition, an equal cost in mixed- vs. single-genotype infections also produced a lower frequency of resistance at high-transmission in the full model, but not in the GI-only model, indicating that within-host competition will exacerbate the disadvantage of resistant parasites under high-transmission, but does not generate the negative correlation. The temporal dynamics of resistance invasion showed that the self-limiting property of resistant parasites creates a specific niche for wild-type infections to coexist. Specifically, as resistance invades, hosts experience more infections, leading to higher generalized immunity. Wild-type infections will then dominate in the lower symptomatic class because they have higher transmissibility.

The inclusion of strain diversity in the model provides a new mechanistic explanation as to why Southeast Asia has been the original source of resistance to certain antimalarial drugs, including chloroquine. In these regions with low strain diversity, parasites cannot repeatedly re-infect hosts. Therefore, clinically immune hosts do not carry infections very often. Thus, in our model resistant strains reach fixation or near-fixation regardless of the actual vectorial capacity, and upon removal of the drug pressure, these regions continue to maintain high levels of drug resistance for a prolonged time. In contrast, high-diversity regions (e.g. Africa) should show a wide range of resistance frequency depending on how antigenic diversity is matched with local vectorial capacities, and should respond more rapidly to changing drug pressures. These results are partially corroborated by a comparison with regions that have higher transmission than Southeast Asia but low diversity (e.g., Papua New Guinea) (***Chen et al., 2011***). The resistance trends for Papua New Guinea behave most similarly to those for Southeast Asia, suggesting that strain diversity, instead of vectorial capacity, is key to predicting trends in drug-resistance frequency.

As comprehensive as the model is, it still has some limitations. First, it currently assumes that resistance is determined by a single locus. If resistance is encoded or augmented by two or more loci (e.g., ACT or SP), past population genetic models demonstrate that rates of recombination could

strongly influence the spread and maintenance of resistance (***Dye and Williams, 1997***; ***Hastings, 2006***). Recent models have shown that pre-existing partner-drug resistant genotypes promote the establishment of Artemisinin resistance (***Watson et al., 2022***). However, as recombination is one of the potential reasons explaining why multilocus resistance has delayed appearance in high-transmission regions, the incorporation of recombination is not expected to alter the negative relationship between resistance and prevalence. These earlier population genetics models of drug resistance posit that a high selfing rate in low transmission ensures high linkage among multilocus resistance, promoting their higher frequencies (***Dye and Williams, 1997***; ***Hastings and D'Alessandro, 2000***; ***Hastings and Donnelly, 2005***). It is thus expected that adding multilocus resistance will augment the negative correlation between resistance and prevalence. Expansion of the current model to include multilocus resistance will shed light on this prediction.

The second potential limitation of our model lies in the assumption that parasites are independently and randomly distributed in hosts, while the negative binomial distribution (NBD) is widely used in macroparasitic models (***Anderson and May, 1978***). Empirical evidence of parasite burdens is usually over-dispersed in that relatively few members of the host population harbor the majority of the parasite population (***Anderson and Gordon, 1982***; ***Churcher et al., 2005***; ***Grogan et al., 2016***). In our model, we argue that despite the MOI within each G class being Poisson distributed, the population-level MOI distribution is over-dispersed as hosts in the $G2$ class are much less likely to be infected than in $G1$ or $G0$ (***Figure 2—figure Supplement 2***) and hosts in drug-treated classes have lower MOI than untreated classes as they harbor mostly resistant parasites only. By discretization of host classes and parasite types, we considered over-dispersion at the population level. Future models could expand on the NBD for individual classes by fitting empirical data from different age classes.

Lastly, our model assumed a random association between resistant genotype and antigenic diversity. In reality, in the early stage of invasion, the resistant genotype should have a limited antigenic background until it becomes widespread. In an agent-based stochastic model, ***Whitlock et al. (2021)*** found that selection for high antigenic variation in high transmission slows the spread of resistance. The interference of immune selection and resistance might serve as an additional reason why resistant parasites are at lower frequencies in high-transmission settings. Future stochastic models are desirable for quantifying the dynamics of interactions between antigenic variation and resistant loci under different epidemiological settings.

It is also to be noted that the trend found in our model predicts an equilibrium state of resistance frequency under persistent drug usage, which cannot be extrapolated to transient dynamics of new drug introduction. As shown in ***Figure 6***, a fast sweeping phase is always associated with a new introduction of resistant genotypes in both low and high diversity regions. Therefore, we focused on empirical comparison to Pfcrt 76T because this mutation is essential for chloroquine resistance (***Ecker et al., 2012***) and chloroquine has been heavily used as first-line drugs for years in most countries.

In sum, we show that strain diversity and associated strain-specific host immunity, dynamically tracked through the macroparasitic structure, can explain the complex relationship between transmission intensity and drug-resistance frequencies. Our model implies that control protocols should vary from region to region and that there is no one-size-fits-all cure for malaria control worldwide (***Rasmussen et al., 2022***). In regions of low prevalence, such as Southeast Asia, long-term goals for malaria prevention will likely not be aided by intensive drug treatment (***Delacollette et al., 2009***; ***Imwong et al., 2020***). In these regions, elimination of falciparum malaria through vector control measures could proceed with little effect on drug resistance levels, whereas continual drug treatment will almost certainly cause fixation or near-fixation of resistance for a prolonged period of time, even after discontinuation of one drug. In contrast, in high prevalence regions such as sub-Saharan Africa, measures of prompt switching between first-line drugs and combination therapies will be quite robust against rapid increases and prolonged maintenance of drug resistance (***Flegg et al., 2013***).

Methods and Materials

Transmission dynamics

Rather than following the infected vector populations, vectorial capacity is given by a fixed contact rate, which represents the contact rate per host at which a mosquito bites a donor host and transmits to a recipient host. This contact rate is uniform across all host classes. Hosts may harbor 0 to n_{max} strains of parasites. Those with $MOI > 0$ will be able to infect mosquitoes. However, a strain from the donor does not guarantee its successful infection in a recipient. Instead, the infections will not result if the host has reached its carrying capacity of n_{max} strains, at which they cannot harbor more infections, or if the host has encountered and acquired the specific immunity to the strain (***Figure 1***A). In these cases, the MOI in the host remains constant. Otherwise, infection will result and MOI is increased by 1.

Calculating Multiplicity of Infection (MOI) and Parasite Prevalence

A major assumption that links host and parasite populations is that the number of infections in an individual host (i.e., MOI) at any time follows some pre-specified distribution. To reduce the number of parameters and simplify the model, a Poisson distribution was used for MOI within a given G and treatment class. This assumption allows us to directly calculate the prevalence (i.e. the fraction of individuals carrying at least one infection) in a given G class $i = 0, 1, 2$ and treatment class $j = U, D$ as

$$I_{i,j} = 1 - \exp(-r_{i,j}) \tag{2}$$

where r is the mean MOI of the class and is equal to

$$r_{i,j} = \frac{PW_{i,j} + PR_{i,j}}{H_{i,j}} \tag{3}$$

Above, $PW_{i,j}$ and $PR_{i,j}$ are the numbers of wild-type (W) and resistant (R) infections circulating in the host class at a given time, and are determined from the system of mechanistic differential equations (***Figure 1—figure Supplement 1*** B). $H_{i,j}$ is the number of hosts in the class at a given time and is similarly determined by the ODE system (***Figure 1—figure Supplement 1*** A).

One justification for using a Poisson distribution for MOI is a reduction in complexity given a lack of knowledge from empirical data; however, the model can be extended to include an implicit clustering if the Poisson distribution is replaced by a negative binomial distribution.

Finally, the population-level prevalence is thus the summation of prevalence in individual host classes,

$$I = \sum_{i,j} I_{i,j} \times (H_{i,j} / \sum H_{i,j}) \tag{4}$$

MOI Dependent Versus MOI Independent Rates

The macroparasite modeling approach also impacts how transition rates are calculated, which is different from typical SIR models. Some transition rates of host classes in the ODE system are dependent on the number of parasite infections (i.e., MOI), whereas some are independent of MOI. For example, host natural death rate ($H_{ij}\alpha$) is MOI-independent because the rate itself need not be weighted by an additional factor related to MOI. Accordingly, parasite death rate due to host natural death is $(PW_{ij} + PR_{ij})\alpha$. Alternatively, host drug treatment rate depends on MOI. The value of this rate is explicitly equal to

$$(G_{i,U} \rightarrow G_{i,D}) = H_{i,U}(t) \sum_{k=1|i,U}^{\infty} k \cdot p(k) d \tag{5}$$

where each k is the number of infections in a given host, $p(k)$ is the fraction of hosts having k infections, and d is the fixed treatment rate upon experiencing symptoms. The reason the second

term is necessary is to count each separate infection as a different chance to experience symptoms. Given that this term is equal to $r_{i,U} = \frac{PW_{i,U}(t)+PR_{i,U}(t)}{H_{i,U}(t)}$, we get that

$$(G_{i,U} \rightarrow G_{i,D}) = (PW_{i,U}(t) + PR_{i,U}(t))d \tag{6}$$

Thus, the movement rates for parasites from untreated classes to drug-treated classes need to consider the host movement rates as well as the number of parasites that are "carried" by the hosts. Using resistant parasites as an example,

$$\begin{aligned}(PR_{i,U} \rightarrow PR_{i,D}) &= H_{i,U}(t) \sum_{k=1|i,U}^{\infty} k \cdot d \cdot k \cdot p(k) \\ &= H_{i,U}(t)E(k^2)d\end{aligned} \tag{7}$$

where $E(k^2)$ refers to the expectation value of the square of the MOI distribution. Given that this expectation value can be written as $var(k) + (E(k))^2$, given the Poisson assumption (which implies that $var(k)$ and $E(k)$ are equal), we finally get an overall rate of

$$(PR_{i,U} \rightarrow PR_{i,D}) = PR_{i,U}(t)(1 + r_{i,U}^{PR})d \tag{8}$$

where $r_{i,U}^{PR}$ is the mean MOI ($E(k)$) of resistant parasites in the $G_{i,U}$ class.

Cost of Resistance and Contributions of Wild-type and Resistant Parasites to Transmission

Also calculated using Poisson statistics are the contributions of the two parasite genotypes to transmission originating from a host in a given G class. These contributions are dependent on two fixed cost parameters - the fitness cost to transmission associated with resistance in the absence of sensitive parasites (s_{single}, for single-genotype), and the fitness cost to transmission associated with resistance due to competition with wild-type parasites present in the same host (s_{mixed}, for mixed-genotype). Parasite density is assumed to be regulated by similar resources within a host (e.g., red blood cells) regardless of MOI. Thus, each strain has a reduced transmissibility when MOI > 1. For wild-type-only infections of MOI= k, each strain has a transmissibility of $1/k$; for resistant-only infections, each strain has a transmissibility of $1/k \cdot (1 - s_{single})$; for mixed-genotype infections, if there are m wild-type strains and n resistant strains, transmission from n resistant strains is $\frac{n}{m+n}(1 - s_{mixed})$, while transmission from m wild-type strains is $\frac{m}{m+n} + \frac{n}{m+n}s_{mixed}$ assuming wild-type strains out-compete resistant strains in growth rates and reach a higher cumulative density during the infective period.

Based on these assumptions, we then calculate transmissibility contributions at the population level from wild-type strains in purely wild-type infections ($\phi_{WS,ij}$), wild-type strains in mixed-genotype infections ($\phi_{WM,ij}$), resistant strains in purely resistant infections ($\phi_{RS,ij}$), and resistant strains in mixed-genotype infections ($\phi_{RM,ij}$). Details on how these terms were calculated using Poisson statistics appear in the ***Appendix 1***. The total contributions to transmissibility from resistant and sensitive parasites at a given time step are then

$$\Omega_{W,ij} = \phi_{WS,ij} + \phi_{WM,ij} + (\phi_{RM,ij})(s_{mixed}) \tag{9}$$

$$\Omega_{R,ij} = (\phi_{RS,ij})(1 - s_{single}) + (\phi_{RM,ij})(1 - s_{mixed}) \tag{10}$$

These contributions can then be used to determine the realized transmission rates given a vectorial capacity, as shown in the ***Appendix 1***.

Describing the Process of Immunity Loss

A significant challenge in developing the model is to describe a function for immunity loss for a given class. We adopted the classic equations for the dynamics of acquired immunity boosted by exposure to infection (Eq. 2.5 from ***Aron*** (***1983***)). This gives the following immunity loss rate from a higher generalized immunity class to a lower one:

$$(G_{i,j} \rightarrow G_{i-1,j}) = h_{i,j} \frac{\exp(-\frac{h_{i,j}}{\Lambda})}{1 - \exp(-\frac{h_{i,j}}{\Lambda})} \tag{11}$$

In this case, $h_{i,j}$ is the sum of the inoculation rate and host death rate for the $G_{i,j}$ class and is determined mechanistically, and Λ is a fixed immunity loss rate parameter with dimensions of $1/[time]$. The second factor in the equation represents the failure of boosting, i.e., the probability that an individual is infected after the period of immunity has ended given that they were not infected within the immune state (***Aron and May, 1982***).

Empirical database and Regression Analysis

We acquired resistance marker *pfcrt* 76T frequencies from the Worldwide Antimalarial Resistance Network (WWARN). The website obtained resistant frequencies from 587 studies between 2001 and 2022 with specific curation methodologies. We then extracted geographic sampling locations from the database, and extracted *Pf* prevalence data estimated from 2-10 years old children from Malaria Atlas Project. The Malaria Atlas Project does not have predicted prevalence before 2000, while the change in first-line antimalarial drugs started around early 2000 in most African countries. We therefore restricted our empirical comparisons of equilibrium levels of resistance and prevalence to studies that conducted surveys between 1990 and 2000 and used estimated prevalence from the year 2000 as the proxy for this sampling period. Studies with a host sampling size of less than 20 were excluded. Data sources on drug usage and policies for different countries are summarized in ***Table 1***.

The relationship between prevalence and resistant frequency was investigated using beta regression because both the explanatory variable and response variable are proportions, restricted to the unit interval (0,1) (***Ferrari and Cribari-Neto, 2004***; ***Simas et al., 2010***). Thus, the proper distribution of the response variable (here, resistant prevalence) should be a beta distribution with a mean and precision parameter. Since resistant frequency also has extremes of 0 and 1, we transformed the frequency data to restrict its range between 0 and 1 first so that beta regression still applies,

$$freq_{adj} = (freq \cdot (n-1) + 0.5)/n \tag{12}$$

where n is the sample size (***Smithson and Verkuilen, 2006***). We then used *betareg* function from R package 4.2.1 *betareg* 3.1-4 to perform the regression (***Cribari-Neto and Zeileis, 2010***).

Table 1. Source of drug policy data.

Country	Citations
Kenya	***Hemming-Schroeder et al.*** (***2018***)
Ghana	***Flegg et al.*** (***2013***)
Cambodia	***Delacollette et al.*** (***2009***)
Thailand	***Delacollette et al.*** (***2009***); ***Rasmussen et al.*** (***2022***)
Papua New Guinea	***Nsanzabana et al.*** (***2010***)
Brazil	***Gama et al.*** (***2009***)

Acknowledgments

We thank Mercedes Pascual for valuable suggestions on earlier versions of the model, and Karen Day and Kathryn Tiedje for their helpful discussions and feedback related to this work. We appreciate the support of Information Technology at Purdue University through the computational resources of the Bell Community Cluster.

Funding

This work was partially supported by the joint NIH-NSF-NIFA Ecology and Evolution of Infectious Disease award R01-AI149779 to Karen Day and Mercedes Pascual.

Data Availability

All the ODE codes, numerically-simulated data, empirical data, and analyzing scripts are publicly available at https://github.itap.purdue.edu/HeLab/MalariaResistance.

References

Alifrangis M, Lemnge MM, Rønn AM, Segeja MD, Magesa SM, Khalil IF, Bygbjerg IC. Increasing prevalence of wildtypes in the dihydrofolate reductase gene of Plasmodium falciparum in an area with high levels of sulfadoxine/pyrimethamine resistance after introduction of treated bed nets. The American Journal of Tropical Medicine and Hygiene. 2003 Sep; 69(3):238–243.

Anderson RM, Gordon DM. Processes influencing the distribution of parasite numbers within host populations with special emphasis on parasite-induced host mortalities. Parasitology. 1982 Oct; 85(2):373–398. http://www.cambridge.org/core/journals/parasitology/article/processes-influencing-the-distribution-of-parasite-numbers-within-host-populations-with-special-emphasis-on-parasiteinduced89A2C5D03D3F8533C63276FA38806396, doi: 10.1017/S0031182000055347, publisher: Cambridge University Press.

Anderson RM, May RM. Regulation and Stability of Host-Parasite Population Interactions: I. Regulatory Processes. Journal of Animal Ecology. 1978; 47(1):219–247. http://www.jstor.org/stable/3933, doi: 10.2307/3933, publisher: [Wiley, British Ecological Society].

Ariey F, Robert V. The puzzling links between malaria transmission and drug resistance. Trends in Parasitology. 2003 Apr; 19(4):158–160. https://www.sciencedirect.com/science/article/pii/S1471492203000540, doi: 10.1016/S1471-4922(03)00054-0.

Aron JL. Dynamics of acquired immunity boosted by exposure to infection. Mathematical Biosciences. 1983 Jun; 64(2):249–259. https://www.sciencedirect.com/science/article/pii/002555648390007X, doi: 10.1016/0025-5564(83)90007-X.

Aron JL, May RM. The population dynamics of malaria. In: Anderson RM, editor. *The Population Dynamics of Infectious Diseases: Theory and Applications* Boston, MA: Springer US; 1982.p. 139–179. http://link.springer.com/10.1007/978-1-4899-2901-3_5, doi: 10.1007/978-1-4899-2901-3_5.

Artzy-Randrup Y, Alonso D, Pascual M. Transmission Intensity and Drug Resistance in Malaria Population Dynamics: Implications for Climate Change. PLOS ONE. 2010 Oct; 5(10):e13588. https://journals.plos.org/plosone/article?id=10.1371/journal.pone.0013588, doi: 10.1371/journal.pone.0013588, publisher: Public Library of Science.

Barry AE, Trieu A, Fowkes FJI, Pablo J, Kalantari-Dehaghi M, Jasinskas A, Tan X, Kayala MA, Tavul L, Siba PM, Day KP, Baldi P, Felgner PL, Doolan DL. The Stability and Complexity of Antibody Responses to the Major Surface Antigen of Plasmodium falciparum Are Associated with Age in a Malaria Endemic Area. Molecular & Cellular Proteomics : MCP. 2011 Nov; 10(11). http://www.ncbi.nlm.nih.gov/pmc/articles/PMC3226400/, doi: 10.1074/mcp.M111.008326.

Best Plummer W, Pinto Pereira LM, Carrington CVF. Pfcrt and pfmdr1 alleles associated with chloroquine resistance in Plasmodium falciparum from Guyana, South America. Memorias Do Instituto Oswaldo Cruz. 2004 Jun; 99(4):389–392. doi: 10.1590/s0074-02762004000400008.

Blasco B, Leroy D, Fidock DA. Antimalarial drug resistance: linking Plasmodium falciparum parasite biology to the clinic. Nature Medicine. 2017 Aug; 23(8):917–928. https://www.nature.com/articles/nm.4381, doi: 10.1038/nm.4381, bandiera_abtest: a Cg_type: Nature Research Journals Number: 8 Primary_atype: Reviews Publisher: Nature Publishing Group Subject_term: Drug therapy;Malaria;Therapeutics Subject_term_id: drug-therapy;malaria;therapeutics.

Bonnet S, Gouagna LC, Paul RE, Safeukui I, Meunier JY, Boudin C. Estimation of malaria transmission from humans to mosquitoes in two neighbouring villages in south Cameroon: evaluation and comparison of several indices. Transactions of the Royal Society of Tropical Medicine and Hygiene. 2003 Jan; 97(1):53–59. https://www.sciencedirect.com/science/article/pii/S0035920303900228, doi: 10.1016/S0035-9203(03)90022-8.

Bull PC, Lowe BS, Kortok M, Marsh K. Antibody Recognition of Plasmodium falciparum Erythrocyte Surface Antigens in Kenya: Evidence for Rare and Prevalent Variants. Infection and Immunity. 1999 Feb; 67(2):733–739. http://iai.asm.org/content/67/2/733.

Bull PC, Lowe BS, Kortok M, Molyneux CS, Newbold CI, Marsh K. Parasite antigens on the infected red cell surface are targets for naturally acquired immunity to malaria. Nature medicine. 1998 Mar; 4(3):358–360. http://www.ncbi.nlm.nih.gov/pmc/articles/PMC3836255/.

Bushman M, Antia R, Udhayakumar V, Roode JCd. Within-host competition can delay evolution of drug resistance in malaria. PLOS Biology. 2018 Aug; 16(8):e2005712. https://journals.plos.org/plosbiology/article?id=10.1371/journal.pbio.2005712, doi: 10.1371/journal.pbio.2005712, publisher: Public Library of Science.

Bushman M, Morton L, Duah N, Quashie N, Abuaku B, Koram KA, Dimbu PR, Plucinski M, Gutman J, Lyaruu P, et al. Within-host competition and drug resistance in the human malaria parasite Plasmodium falciparum. Proceedings of the Royal Society B: Biological Sciences. 2016; 283(1826):20153038.

Chaijaroenkul W, Ward SA, Mungthin M, Johnson D, Owen A, Bray PG, Na-Bangchang K. Sequence and gene expression of chloroquine resistance transporter (pfcrt) in the association of in vitro drugs resistance of Plasmodium falciparum. Malaria Journal. 2011 Feb; 10(1):42. https://doi.org/10.1186/1475-2875-10-42, doi: 10.1186/1475-2875-10-42.

Chen DS, Barry AE, Leliwa-Sytek A, Smith TA, Peterson I, Brown SM, Migot-Nabias F, Deloron P, Kortok MM, Marsh K, Daily JP, Ndiaye D, Sarr O, Mboup S, Day KP. A Molecular Epidemiological Study of var Gene Diversity to Characterize the Reservoir of Plasmodium falciparum in Humans in Africa. PLOS ONE. 2011 Feb; 6(2):e16629. https://journals.plos.org/plosone/article?id=10.1371/journal.pone.0016629, doi: 10.1371/journal.pone.0016629.

Churcher T, Ferguson N, Basanez MG. Density dependence and overdispersion in the transmission of helminth parasites. Parasitology. 2005; 131(1):121–132.

Collins WE, Jeffery GM. A retrospective examination of sporozoite-and trophozoite-induced infections with Plasmodium falciparum in patients previously infected with heterologous species of Plasmodium: effect on development of parasitologic and clinical immunity. The American journal of tropical medicine and hygiene. 1999; 61(1_Supplement):36–43.

Cribari-Neto F, Zeileis A. Beta Regression in R. Journal of Statistical Software. 2010; 34(2):1–24. doi: 10.18637/jss.v034.i02.

Curtis CF, Otoo LN. A simple model of the build-up of resistance to mixtures of anti-malarial drugs. Transactions of the Royal Society of Tropical Medicine and Hygiene. 1986 Jan; 80(6):889–892. https://www.sciencedirect.com/science/article/pii/0035920386902488, doi: 10.1016/0035-9203(86)90248-8.

Day KP, Marsh K. Naturally acquired immunity to Plasmodium falciparum. Immunology Today. 1991 Jan; 12(3):A68–A71. http://www.sciencedirect.com/science/article/pii/S0167569905800209, doi: 10.1016/S0167-5699(05)80020-9.

De Roode JC, Helinski ME, Anwar MA, Read AF. Dynamics of multiple infection and within-host competition in genetically diverse malaria infections. The American Naturalist. 2005; 166(5):531–542.

Delacollette C, D'Souza C, Christophel E, Thimasarn K, Abdur R, Bell D, Dai TC, Gopinath D, Lu S, Mendoza R, Ortega L, Rastogi R, Tantinimitkul C, Ehrenberg J. MALARIA TRENDS AND CHALLENGES IN THE GREATER MEKONG SUBREGION. SOUTHEAST ASIAN J TROP MED PUBLIC HEALTH. 2009; 40(4):19.

Diallo D, Sutherland C, Nebie I, Konaté A, Ord R, Pota H, Roper C, Ilboudo-Sanogo E, Greenwood B, Cousens S. Sustained use of insecticide-treated curtains is not associated with greater circulation of drug-resistant malaria parasites, or with higher risk of treatment failure among children with uncomplicated malaria in Burkina Faso. The American journal of tropical medicine and hygiene. 2007 Mar; 76:237–44. doi: 10.4269/ajtmh.2007.76.237.

Dietz K, Molineaux L, Thomas A. A malaria model tested in the African savannah. Bulletin of the World Health Organization. 1974; 50(3-4):347–357. https://www.ncbi.nlm.nih.gov/pmc/articles/PMC2481186/.

Djimdé AA, Doumbo OK, Traore O, Guindo AB, Kayentao K, Diourte Y, Niare-Doumbo S, Coulibaly D, Kone AK, Cissoko Y, Tekete M, Fofana B, Dicko A, Diallo DA, Wellems TE, Kwiatkowski D, Plowe CV. Clearance of drug-resistant parasites as a model for protective immunity in Plasmodium falciparum malaria. The American Journal of Tropical Medicine and Hygiene. 2003 Nov; 69(5):558–563.

Dondorp AM, Nosten F, Yi P, Das D, Phyo AP, Tarning J, Lwin KM, Ariey F, Hanpithakpong W, Lee SJ, Ringwald P, Silamut K, Imwong M, Chotivanich K, Lim P, Herdman T, An SS, Yeung S, Singhasivanon P, Day NPJ, et al. Artemisinin Resistance in Plasmodium falciparum Malaria. New England Journal of Medicine. 2009 Jul; 361(5):455–467. https://doi.org/10.1056/NEJMoa0808859, doi: 10.1056/NEJMoa0808859, publisher: Massachusetts Medical Society _eprint: https://doi.org/10.1056/NEJMoa0808859.

Dye C, Williams BG. Multigenic drug resistance among inbred malaria parasites. Proceedings of the Royal Society of London Series B: Biological Sciences. 1997 Jan; 264(1378):61–67. https://royalsocietypublishing.org/doi/abs/10.1098/rspb.1997.0009, doi: 10.1098/rspb.1997.0009, publisher: Royal Society.

Ecker A, Lehane AM, Clain J, Fidock DA. PfCRT and its role in antimalarial drug resistance. Trends in Parasitology. 2012; 28(11):504–514. https://www.sciencedirect.com/science/article/pii/S1471492212001420, doi: https://doi.org/10.1016/j.pt.2012.08.002.

ETHZentrum N. Linking evolutionary ecology with epidemiology. Revue suisse de zoologie. 1994; 101(4):865–874.

Ferrari S, Cribari-Neto F. Beta regression for modelling rates and proportions. Journal of applied statistics. 2004; 31(7):799–815.

Flegg JA, Metcalf CJE, Gharbi M, Venkatesan M, Shewchuk T, Hopkins Sibley C, Guerin PJ. Trends in Antimalarial Drug Use in Africa. The American Journal of Tropical Medicine and Hygiene. 2013 Nov; 89(5):857–865. https://www.ncbi.nlm.nih.gov/pmc/articles/PMC3820326/, doi: 10.4269/ajtmh.13-0129.

Gama BE, de Oliveira NKA, Zalis MG, de Souza JM, Santos F, Daniel-Ribeiro CT, Ferreira-da Cruz MdF. Chloroquine and sulphadoxine-pyrimethamine sensitivity of Plasmodium falciparum parasites in a Brazilian endemic area. Malaria journal. 2009; 8(1):1–5.

Garrett-Jones C, Shidrawi G. Malaria vectorial capacity of a population of Anopheles gambiae: an exercise in epidemiological entomology. Bulletin of the World Health Organization. 1969; 40(4):531.

Grogan LF, Phillott AD, Scheele BC, Berger L, Cashins SD, Bell SC, Puschendorf R, Skerratt LF. Endemicity of chytridiomycosis features pathogen overdispersion. Journal of Animal Ecology. 2016; 85(3):806–816.

Harrington W, Mutabingwa T, Muehlenbachs A, Sorensen B, Bolla M, Fried M, Duffy P. Competitive facilitation of drug-resistant Plasmodium falciparum malaria parasites in pregnant women who receive preventive treatment. Proceedings of the National Academy of Sciences. 2009; 106(22):9027–9032.

Hastings IM. A model for the origins and spread of drug-resistant malaria. Parasitology. 1997 Aug; 115(2):133–141. https://www.cambridge.org/core/journals/parasitology/article/model-for-the-origins-and-spread-of-drugresistant-malaria/FFEAC1AC6D63172567A5FD1BA9731BBF/core-reader, doi: 10.1017/S0031182097001261.

Hastings IM. Complex dynamics and stability of resistance to antimalarial drugs. Parasitology. 2006 May; 132(5):615–624. https://www.cambridge.org/core/journals/parasitology/article/abs/complex-dynamics-and-stability-of-resistance-to-antimalarial-drugs/97DEC52EEA77394F730F4DCC3B501758, doi: 10.1017/S0031182005009790, publisher: Cambridge University Press.

Hastings IM, D'Alessandro U. Modelling a Predictable Disaster:: The Rise and Spread of Drug-resistant Malaria. Parasitology Today. 2000 Aug; 16(8):340–347. https://www.sciencedirect.com/science/article/pii/S0169475800017075, doi: 10.1016/S0169-4758(00)01707-5.

Hastings IM, Donnelly MJ. The impact of antimalarial drug resistance mutations on parasite fitness, and its implications for the evolution of resistance. Drug Resistance Updates. 2005 Feb; 8(1):43–50. http://www.sciencedirect.com/science/article/pii/S1368764605000221, doi: 10.1016/j.drup.2005.03.003.

Hastings IM, Watkins WM, White NJ. The Evolution of Drug-Resistant Malaria: The Role of Drug Elimination Half-Life. Philosophical Transactions: Biological Sciences. 2002; 357(1420):505–519. http://www.jstor.org/stable/3066761, publisher: The Royal Society.

He Q, Pilosof S, Tiedje KE, Day KP, Pascual M. Frequency-Dependent Competition Between Strains Imparts Persistence to Perturbations in a Model of Plasmodium falciparum Malaria Transmission. Frontiers in Ecology and Evolution. 2021; 9:319. https://www.frontiersin.org/article/10.3389/fevo.2021.633263, doi: 10.3389/fevo.2021.633263.

He Q, Pilosof S, Tiedje KE, Ruybal-Pesántez S, Artzy-Randrup Y, Baskerville EB, Day KP, Pascual M. Networks of genetic similarity reveal non-neutral processes shape strain structure in Plasmodium falciparum. Nature Communications. 2018 May; 9(1):1817. https://www.nature.com/articles/s41467-018-04219-3, doi: 10.1038/s41467-018-04219-3.

Hemming-Schroeder E, Umukoro E, Lo E, Fung B, Tomás-Domingo P, Zhou G, Zhong D, Dixit A, Atieli H, Githeko A, Vardo-Zalik A, Yan G. Impacts of Antimalarial Drugs on Plasmodium falciparum Drug Resistance Markers, Western Kenya, 2003–2015. The American Journal of Tropical Medicine and Hygiene. 2018 Mar; 98(3):692–699. https://www.ncbi.nlm.nih.gov/pmc/articles/PMC5930917/, doi: 10.4269/ajtmh.17-0763.

Henden L, Lee S, Mueller I, Barry A, Bahlo M. Identity-by-descent analyses for measuring population dynamics and selection in recombining pathogens. PLoS genetics. 2018; 14(5):e1007279.

Imwong M, Dhorda M, Myo Tun K, Thu AM, Phyo AP, Proux S, Suwannasin K, Kunasol C, Srisutham S, Duanguppama J, Vongpromek R, Promnarate C, Saejeng A, Khantikul N, Sugaram R, Thanapongpichat S, Sawangjaroen N, Sutawong K, Han KT, Htut Y, et al. Molecular epidemiology of resistance to antimalarial drugs in the Greater Mekong subregion: an observational study. The Lancet Infectious Diseases. 2020 Dec; 20(12):1470–1480. https://www.sciencedirect.com/science/article/pii/S1473309920302280, doi: 10.1016/S1473-3099(20)30228-0.

Klein EY, Smith DL, Boni MF, Laxminarayan R. Clinically immune hosts as a refuge for drug-sensitive malaria parasites. Malaria Journal. 2008 Apr; 7(1):67. https://doi.org/10.1186/1475-2875-7-67, doi: 10.1186/1475-2875-7-67.

Klein EY, Smith DL, Laxminarayan R, Levin S. Superinfection and the evolution of resistance to antimalarial drugs. Proceedings of the Royal Society B: Biological Sciences. 2012 Sep; 279(1743):3834–3842. https://royalsocietypublishing.org/doi/full/10.1098/rspb.2012.1064, doi: 10.1098/rspb.2012.1064, publisher: Royal Society.

Koella JC. Costs and Benefits of Resistance against Antimalarial Drugs. Parasitology Today. 1998 Sep; 14(9):360–364. https://www.sciencedirect.com/science/article/pii/S0169475898012976, doi: 10.1016/S0169-4758(98)01297-6.

Koella J, Antia R. Epidemiological models for the spread of anti-malarial resistance. Malaria Journal. 2003 Feb; 2(1):3. https://doi.org/10.1186/1475-2875-2-3, doi: 10.1186/1475-2875-2-3.

Labbé F, He Q, Zhan Q, Tiedje KE, Argyropoulos DC, Tan MH, Ghansah A, Day KP, Pascual M. Neutral vs. non-neutral genetic footprints of Plasmodium falciparum multiclonal infections. PLOS Computational Biology. 2023; 19(1):e1010816.

Lanteri CA, Chaorattanakawee S, Lon C, Saunders DL, Rutvisuttinunt W, Yingyuen K, Bathurst I, Ding XC, Tyner SD. Ex Vivo Activity of Endoperoxide Antimalarials, Including Artemisone and Arterolane, against Multidrug-Resistant Plasmodium falciparum Isolates from Cambodia. Antimicrobial Agents and Chemotherapy. 2014 Oct; 58(10):5831–5840. https://journals.asm.org/doi/full/10.1128/AAC.02462-14, doi: 10.1128/AAC.02462-14, publisher: American Society for Microbiology.

Maire N, Smith T, Ross A, Owusu-Agyei S, Dietz K, Molineaux L. A model for natural immunity to asexual blood stages of Plasmodium falciparum malaria in endemic areas. The American journal of tropical medicine and hygiene. 2006; 75(2 Supp):19–31.

Masserey T, Lee T, Golumbeanu M, Shattock AJ, Kelly SL, Hastings IM, Penny MA. The influence of biological, epidemiological, and treatment factors on the establishment and spread of drug-resistant Plasmodium falciparum. Elife. 2022; 11:e77634.

Mharakurwa S, Mutambu SL, Mudyiradima R, Chimbadzwa T, Chandiwana SK, Day KP. Association of house spraying with suppressed levels of drug resistance in Zimbabwe. Malaria Journal. 2004 Oct; 3(1):35. https://doi.org/10.1186/1475-2875-3-35, doi: 10.1186/1475-2875-3-35.

Molineaux L, Gramiccia G, Organization WH, et al. The Garki project: research on the epidemiology and control of malaria in the Sudan savanna of West Africa. World Health Organization; 1980.

Myers-Hansen JL, Abuaku B, Oyebola MK, Mensah BA, Ahorlu C, Wilson MD, Awandare G, Koram KA, Ngwa AA, Ghansah A. Assessment of antimalarial drug resistant markers in asymptomatic Plasmodium falciparum infections after 4 years of indoor residual spraying in Northern Ghana. PLOS ONE. 2020 Dec; 15(12):e0233478. https://journals.plos.org/plosone/article?id=10.1371/journal.pone.0233478, doi: 10.1371/journal.pone.0233478, publisher: Public Library of Science.

Narh CA, Ghansah A, Duffy MF, Ruybal-Pesántez S, Onwona CO, Oduro AR, Koram KA, Day KP, Tiedje KE. Evolution of Antimalarial Drug Resistance Markers in the Reservoir of Plasmodium falciparum Infections in the Upper East Region of Ghana. The Journal of Infectious Diseases. 2020 Oct; 222(10):1692–1701. https://doi.org/10.1093/infdis/jiaa286, doi: 10.1093/infdis/jiaa286.

Nkhoma SC, Trevino SG, Gorena KM, Nair S, Khoswe S, Jett C, Garcia R, Daniel B, Dia A, Terlouw DJ, Ward SA, Anderson TJ, Cheeseman IH. Resolving within-host malaria parasite diversity using single-cell sequencing. bioRxiv. 2018 Aug; p. 391268. https://www.biorxiv.org/content/early/2018/08/13/391268, doi: 10.1101/391268.

Noedl H, Se Y, Schaecher K, Smith BL, Socheat D, Fukuda MM. Evidence of Artemisinin-Resistant Malaria in Western Cambodia. New England Journal of Medicine. 2008 Dec; 359(24):2619–2620. https://doi.org/10.1056/NEJMc0805011, doi: 10.1056/NEJMc0805011, publisher: Massachusetts Medical Society _eprint: https://doi.org/10.1056/NEJMc0805011.

Nsanzabana C, Hastings IM, Marfurt J, Muüller I, Baea K, Baea K, Rare L, Schapira A, Felger I, Betschart B, et al. Quantifying the evolution and impact of antimalarial drug resistance: drug use, spread of resistance, and drug failure over a 12-year period in Papua New Guinea. The Journal of infectious diseases. 2010; 201(3):435–443.

Pilosof S, He Q, Tiedje KE, Ruybal-Pesántez S, Day KP, Pascual M. Competition for hosts modulates vast antigenic diversity to generate persistent strain structure in Plasmodium falciparum. PLOS Biology. 2019 Jun; 17(6):e3000336. https://journals.plos.org/plosbiology/article?id=10.1371/journal.pbio.3000336, doi: 10.1371/journal.pbio.3000336.

R Core Team. R: A Language and Environment for Statistical Computing. R Foundation for Statistical Computing, Vienna, Austria; 2023, https://www.R-project.org/.

Rask TS, Hansen DA, Theander TG, Pedersen AG, Lavstsen T. Plasmodium falciparum Erythrocyte Membrane Protein 1 Diversity in Seven Genomes – Divide and Conquer. PLOS Computational Biology. 2010 Sep; 6(9):e1000933. http://journals.plos.org/ploscompbiol/article?id=10.1371/journal.pcbi.1000933, doi: 10.1371/journal.pcbi.1000933.

Rasmussen C, Alonso P, Ringwald P. Current and emerging strategies to combat antimalarial resistance. Expert Review of Anti-infective Therapy. 2022 Mar; 20(3):353–372. https://doi.org/10.1080/14787210.2021.1962291, doi: 10.1080/14787210.2021.1962291, publisher: Taylor & Francis _eprint: https://doi.org/10.1080/14787210.2021.1962291.

de Roode JC, Culleton R, Bell AS, Read AF. Competitive release of drug resistance following drug treatment of mixed Plasmodium chabaudi infections. Malaria Journal. 2004 Sep; 3(1):33. https://doi.org/10.1186/1475-2875-3-33, doi: 10.1186/1475-2875-3-33.

Ruybal-Pesántez S, Tiedje KE, Pilosof S, Tonkin-Hill G, He Q, Rask TS, Amenga-Etego L, Oduro AR, Koram KA, Pascual M, Day KP. Age-specific patterns of DBLα var diversity can explain why residents of high malaria transmission areas remain susceptible to Plasmodium falciparum blood stage infection throughout life. International Journal for Parasitology. 2022 Jan; https://www.sciencedirect.com/science/article/pii/S0020751922000030, doi: 10.1016/j.ijpara.2021.12.001.

Shah M, Kariuki S, Eng JV, Blackstock AJ, Garner K, Gatei W, Gimnig JE, Lindblade K, Terlouw D, Kuile Ft, Hawley WA, Phillips-Howard P, Nahlen B, Walker E, Hamel MJ, Slutsker L, Shi YP. Effect of Transmission Reduction by Insecticide-Treated Bednets (ITNs) on Antimalarial Drug Resistance in Western Kenya. PLOS ONE. 2011 Nov; 6(11):e26746. https://journals.plos.org/plosone/article?id=10.1371/journal.pone.0026746, doi: 10.1371/journal.pone.0026746, publisher: Public Library of Science.

Shah M, Omosun Y, Lal A, Odero C, Gatei W, Otieno K, Gimnig JE, Kuile Ft, Hawley WA, Nahlen B, Kariuki S, Walker E, Slutsker L, Hamel M, Shi YP. Assessment of molecular markers for anti-malarial drug resistance after the introduction and scale-up of malaria control interventions in western Kenya. Malaria Journal. 2015 Feb; 14(1):75. https://doi.org/10.1186/s12936-015-0588-4, doi: 10.1186/s12936-015-0588-4.

Simas AB, Barreto-Souza W, Rocha AV. Improved estimators for a general class of beta regression models. Computational Statistics & Data Analysis. 2010; 54(2):348–366.

Smithson M, Verkuilen J. A better lemon squeezer? Maximum-likelihood regression with beta-distributed dependent variables. Psychological methods. 2006; 11(1):54.

Soetaert K, Petzoldt T, Setzer RW. Solving Differential Equations in R: Package deSolve. Journal of Statistical Software. 2010; 33(9):1–25. doi: 10.18637/jss.v033.i09.

Talisuna AO, Langi P, Bakyaita N, Egwang T, Mutabingwa TK, Watkins W, Van Marck E, D'Alessandro U. Intensity of malaria transmission, antimalarial-drug use and resistance in Uganda: what is the relationship between these three factors? Transactions of the Royal Society of Tropical Medicine and Hygiene. 2002 May; 96(3):310–317. https://www.sciencedirect.com/science/article/pii/S0035920302901082, doi: 10.1016/S0035-9203(02)90108-2.

Tiedje KE, Oduro AR, Agongo G, Anyorigiya T, Azongo D, Awine T, Ghansah A, Pascual M, Koram KA, Day KP. Seasonal Variation in the Epidemiology of Asymptomatic Plasmodium falciparum Infections across Two Catchment Areas in Bongo District, Ghana. The American Journal of Tropical Medicine and Hygiene. 2017 Jul; 97(1):199–212. http://www.ajtmh.org/content/journals/10.4269/ajtmh.16-0959, doi: 10.4269/ajtmh.16-0959.

Tonkin-Hill GQ, Trianty L, Noviyanti R, Nguyen HHT, Sebayang BF, Lampah DA, Marfurt J, Cobbold SA, Rambhatla JS, McConville MJ, Rogerson SJ, Brown GV, Day KP, Price RN, Anstey NM, Papenfuss AT, Duffy MF. The Plasmodium falciparum transcriptome in severe malaria reveals altered expression of genes involved in important processes including surface antigen–encoding var genes. PLOS Biology. 2018 Mar; 16(3):e2004328. http://journals.plos.org/plosbiology/article?id=10.1371/journal.pbio.2004328, doi: 10.1371/journal.pbio.2004328.

Volkman SK, Barry AE, Lyons EJ, Nielsen KM, Thomas SM, Choi M, Thakore SS, Day KP, Wirth DF, Hartl DL. Recent Origin of Plasmodium falciparum from a Single Progenitor. Science. 2001 Jul; 293(5529):482–484. https://www.science.org/doi/full/10.1126/science.1059878, doi: 10.1126/science.1059878, publisher: American Association for the Advancement of Science.

Watson OJ, Gao B, Nguyen TD, Tran TNA, Penny MA, Smith DL, Okell L, Aguas R, Boni MF. Pre-existing partner-drug resistance to artemisinin combination therapies facilitates the emergence and spread of artemisinin resistance: a consensus modelling study. The Lancet Microbe. 2022; 3(9):e701–e710.

Whitlock AOB, Juliano JJ, Mideo N. Immune selection suppresses the emergence of drug resistance in malaria parasites but facilitates its spread. PLOS Computational Biology. 2021 Jul; 17(7):e1008577. https://journals.plos.org/ploscompbiol/article?id=10.1371/journal.pcbi.1008577, doi: 10.1371/journal.pcbi.1008577, publisher: Public Library of Science.

Wickham H. ggplot2: Elegant Graphics for Data Analysis. Springer-Verlag New York; 2016. https://ggplot2.tidyverse.org.

Wickham H, Averick M, Bryan J, Chang W, McGowan LD, François R, Grolemund G, Hayes A, Henry L, Hester J, Kuhn M, Pedersen TL, Miller E, Bache SM, Müller K, Ooms J, Robinson D, Seidel DP, Spinu V, Takahashi K, et al. Welcome to the tidyverse. Journal of Open Source Software. 2019; 4(43):1686. doi: 10.21105/joss.01686.

zur Wiesch PA, Kouyos R, Engelstädter J, Regoes RR, Bonhoeffer S. Population biological principles of drug-resistance evolution in infectious diseases. The Lancet Infectious Diseases. 2011 Mar; 11(3):236–247. https://www.sciencedirect.com/science/article/pii/S1473309910702644, doi: 10.1016/S1473-3099(10)70264-4.

Wong W, Griggs AD, Daniels RF, Schaffner SF, Ndiaye D, Bei AK, Deme AB, MacInnis B, Volkman SK, Hartl DL, et al. Genetic relatedness analysis reveals the cotransmission of genetically related Plasmodium falciparum parasites in Thiès, Senegal. Genome Medicine. 2017; 9(1):1–12.

Appendix 1

Basic Model Structure

The primary structure of the macroparasitic model is composed of three submodels: (i) the number of hosts in generalized immunity classes, (ii) circulating infections (parasites) in host GI classes, and (iii) the dynamics of immune memory of host GI classes (***Figure 1—figure Supplement 1***; list of parameters: ***Appendix 1***-Table 1). These submodels are interconnected: the infectivity of new parasites is determined by the accumulated immune memory in the different host classes; some of the transition rates of host classes are dependent on the number of parasite infections (i.e., MOI), whereas some are independent of MOI; While the transition rates of resistant or wild-type parasites between untreated host classes are identical, they experience vastly different survival rates in treated classes.

The host submodel divides human hosts into three generalized immunity classes, dubbed class G_0, class G_1, and class G_2. These immunity classes are defined by the extent to which generalized immunity causes them to experience symptoms, as well as the severity of those symptoms. Each immunity class is further separated into drug-treated (D) and untreated (U) classes. The populations of hosts in the different immune classes are denoted by $H_{0,U}$, $H_{0,D}$, $H_{1,U}$, $H_{1,D}$, $H_{2,U}$, and $H_{2,D}$. The total host population is referred to as H and the total number of extant infections in the population is P.

Parasites are categorized according to their genotype and associated host classes, in which PW and PR denote wild-type and resistant parasite populations, respectively. With the associated host generalized immunity class structure, the parasite classes are further subdivided into $PW_{0,U}$, $PW_{0,D}$, $PW_{1,U}$, $PW_{1,D}$, $PW_{2,U}$, $PW_{2,D}$, $PR_{0,U}$, $PR_{0,D}$, $PR_{1,U}$, $PR_{1,D}$, $PR_{2,U}$, and $PR_{2,D}$.

We assume parasites follow a Poisson distribution within each host class. Therefore, the prevalence (i.e., the fraction of individuals carrying at least one infection) in a given G class $i = 0, 1, 2$ and treatment class $j = U, D$ is,

$$I_{i,j} = 1 - \exp(-r_{i,j}) \tag{13}$$

where r is the mean MOI (parasite-to-host ratio) of the class and is equal to

$$r_{i,j} = \frac{PW_{i,j} + PR_{i,j}}{H_{i,j}} \tag{14}$$

Thus, the overall population-level prevalence is

$$I = \sum_{i,j} I_{i,j} \times (H_{i,j} / \sum H_{i,j}) \tag{15}$$

Further using the Poisson assumption, the proportions of hosts in each class that have no sensitive parasites are

$$p_{0_{W,ij}} = e^{-r_{i,j} \frac{PW_{i,j}}{PW_{i,j}+PR_{i,j}}} \tag{16}$$

The equivalent values for the proportions of hosts in each class that have no resistant parasites are

$$p_{0_{R,ij}} = e^{-r_{i,j} \frac{PR_{i,j}}{PW_{i,j}+PR_{i,j}}} \tag{17}$$

Given these proportions, we can calculate the transmissibility contributions from wild-type strains in purely wild-type infections ($\phi_{WS,ij}$), wild-type strains in mixed-genotype infections ($\phi_{WM,ij}$), resistant strains in purely resistant infections ($\phi_{RS,ij}$), and resistant strains in mixed-genotype infections ($\phi_{RM,ij}$):

$$\phi_{WS,ij} = (1 - p_{0_{W,ij}})p_{0_{R,ij}} \tag{18}$$

$$\phi_{WM,ij} = (1 - p_{0_{W,ij}})(1 - p_{0_{R,ij}})\frac{PW_{i,j}}{PW_{i,j} + PR_{i,j}} \tag{19}$$

$$\phi_{RS,ij} = (1 - p_{0_{R,ij}})p_{0_{W,ij}} \tag{20}$$

$$\phi_{RM,ij} = (1 - p_{0_{W,ij}})(1 - p_{0_{R,ij}})\frac{PR_{i,j}}{PW_{i,j} + PR_{i,j}} \tag{21}$$

The total converted contributions of W and R to transmissibility are therefore

$$\Omega_{W,ij} = \phi_{WS,ij} + \phi_{WM,ij} + (\phi_{RM,ij})(s_{mixed}) \tag{22}$$

$$\Omega_{R,ij} = (\phi_{RS,ij})(1 - s_{single}) + (\phi_{RM,ij})(1 - s_{mixed}) \tag{23}$$

where s_{single} is the fitness cost to transmission associated with resistance in the absence of wild-type parasites and s_{mixed} is the fitness cost to transmission associated with resistance due to competition with wild-type parasites present in the same host. Note that it is assumed that any loss in transmissibility to the resistant parasites due to the mixed cost is recovered by an increase in transmissibility in the co-occurring wild-type parasites.

For the fixed biting rate parameter b, the transmissibilities of wild type and resistant parasites on the whole are therefore

$$\begin{cases} B_{PW} = \frac{b}{H}\sum_{i,j}\Omega_{W,ij}H_{i,j} \\ B_{PR} = \frac{b}{H}\sum_{i,j}\Omega_{R,ij}H_{i,j} \end{cases} \tag{24}$$

The per capita biting rate for untreated hosts is simply

$$B_U = B_{PW} + B_{PR} \tag{25}$$

It is assumed that drug treated hosts can only be infected by resistant parasites, so the effective per capita biting rate for drug-treated hosts is

$$B_D = B_{PR} \tag{26}$$

A unique feature of the first generalized immunity class ($i = 0$) in our model is that there is a significant death rate from the disease, termed $\mu_{0,U}$ or $\mu_{0,D}$. Once a host has moved from the first to the second immune stage, their chance of experiencing symptoms is determined by their specific immunity. Finally, in the third immune class, the hosts can only experience symptoms when a sufficiently distinct migrant strain enters the population (at probability ω).

Given the generalized immunity tracked in each host class, the degree of specific immunity per class is determined as the infectivity of new infection to that class,

$$\eta_i = (1 - \frac{1}{n_{strains}})^{v_i} \tag{27}$$

where $n_{strains}$ represents the number of strains in the local population and v for a given class i refers to the generalized immunity of that class (in terms of the number of infections experienced by an average individual currently in class i). η_i therefore calculates the probability that the host in that G class has not seen a particular strain.

In the following sections, we list how transition rates are calculated in the submodels. Each rate is uniquely marked with the submodel letter and a number, as notated on ***Figure 1—figure Supplement 1***.

Host Submodel

The transition rates between compartments in the host model use the following rates:

Birth

$$\left\{ A1 = \delta \right. \tag{28}$$

where δ is the constant birth rate (into G_{0_U}).

Malarial Death

$$\left\{ \begin{array}{l} A2 = \mu_{0,U} H_{0,U} \\ A3 = \mu_{0,D} H_{0,D} \end{array} \right. \tag{29}$$

Natural Death

$$\left\{ \begin{array}{l} A4 = \alpha H_{0,U} \\ A5 = \alpha H_{0,D} \\ A6 = \alpha H_{1,U} \\ A7 = \alpha H_{1,D} \\ A8 = \alpha H_{2,U} \\ A9 = \alpha H_{2,D} \end{array} \right. \tag{30}$$

where α is the non-disease death rate for the host population.

Drug Treatment of Symptomatic Individuals (MOI-dependent)

$$\left\{ \begin{array}{l} A10 = r_{0,U} d_0 H_{0,U} \\ A11 = r_{1,U} d_1 H_{1,U} \\ A12 = r_{2,U} d_2 \frac{\omega}{n_{strains}} H_{2,U} \end{array} \right. \tag{31}$$

where d_i is the daily treatment rate of hosts in a given class who are currently experiencing symptoms.

Loss of Drug Effectiveness

$$\left\{ \begin{array}{l} A13 = \frac{H_{0,D}}{\tau} \\ A14 = \frac{H_{1,D}}{\tau} \\ A15 = \frac{H_{2,D}}{\tau} \end{array} \right. \tag{32}$$

where τ is the period of drug effectiveness.

Gain of Generalized Immunity

$$\left\{ \begin{array}{l} A16 = (B_U(1 - \frac{r_{0,U}}{K})\rho_1(1 - \eta_0) + \rho_1 r_{0,U} \mu_{PW_U}) H_{0,U} \\ A17 = (B_D(1 - \frac{r_{0,D}}{K})\rho_1(1 - \eta_0) + \rho_1 r_{0,D} \mu_{PR_D}) H_{0,D} \\ A18 = (B_U(1 - \frac{r_{1,U}}{K})\rho_2(1 - \eta_1) + \rho_2 r_{1,U} \mu_{PW_U}) H_{1,U} \\ A19 = (B_D(1 - \frac{r_{1,D}}{K})\rho_2(1 - \eta_1) + \rho_2 r_{1,D} \mu_{PR_D}) H_{1,D} \end{array} \right. \tag{33}$$

where K is the per-host carrying capacity for infections, ρ_1 is the rate of gaining generalized immunity from class 0 to class 1, ρ_2 is the rate of gain of generalized immunity from class 1 to class 2, and μ_{PW_U}, etc. are the parasite clearance rates in different host treatment categories. The first part of the rate indicates that the host receives a previous-seen infection, so it will not result in a new infection, instead, the G is boosted by 1. The second part of the rate indicates that as current infections in the host class are being cleared, G is also boosted.

Loss of Generalized Immunity

$$\begin{cases} A20 = H_{1,U} h_{1,U} \frac{\exp(-\frac{h_{1,U}}{\Lambda})}{1-\exp(-\frac{h_{1,U}}{\Lambda})} \\ A21 = H_{1,D} h_{1,D} \frac{\exp(-\frac{h_{1,D}}{\Lambda})}{1-\exp(-\frac{h_{1,D}}{\Lambda})} \\ A22 = H_{2,U} h_{2,U} \frac{\exp(-\frac{h_{2,U}}{\Lambda})}{1-\exp(-\frac{h_{2,U}}{\Lambda})} \\ A23 = H_{2,D} h_{2,D} \frac{\exp(-\frac{h_{2,D}}{\Lambda})}{1-\exp(-\frac{h_{2,D}}{\Lambda})} \end{cases} \tag{34}$$

$$\begin{cases} h_{1,U} = (B_U(1 - \frac{r_{1,U}}{K})) + \alpha \\ h_{1,D} = (B_D(1 - \frac{r_{1,D}}{K})) + \alpha \\ h_{2,U} = (B_U(1 - \frac{r_{2,U}}{K})) + \alpha \\ h_{2,D} = (B_D(1 - \frac{r_{2,D}}{K})) + \alpha \end{cases} \tag{35}$$

where $Lambda$ is the immunity loss rate. The immunity loss rates follow ***Aron*** (***1983***)'s formulation.

Therefore, ODEs for the host submodel are

$$\begin{cases} \frac{dH_{0,U}}{dt} = (A1) + (A20) + (A13) - (A10) - (A16) - (A2) - (A4) \\ \frac{dH_{0,D}}{dt} = (A21) + (A10) - (A13) - (A17) - (A3) - (A5) \\ \frac{dH_{1,U}}{dt} = (A22) + (A14) + (A16) - (A11) - (A18) - (A20) - (A6) \\ \frac{dH_{1,D}}{dt} = (A23) + (A11) + (A17) - (A14) - (A19) - (A21) - (A7) \\ \frac{dH_{2,U}}{dt} = (A18) + (A15) - (A12) - (A22) - (A8) \\ \frac{dH_{2,D}}{dt} = (A19) + (A12) - (A15) - (A23) - (A9) \end{cases} \tag{36}$$

Parasite Submodel

For the parasite submodel, it is necessary to define a new set of rates, which are mostly variations on the rates from the host submodel:

Infection Via Vector

$$\begin{cases} BW1 = B_{PW} H_{0,U} \eta_0 (1 - \frac{r_{0,U}}{K}) \\ BW2 = B_{PW} H_{1,U} \eta_1 (1 - \frac{r_{1,U}}{K}) \\ BW3 = B_{PW} H_{2,U} \eta_2 (1 - \frac{r_{2,U}}{K}) \end{cases} \tag{37}$$

Transition due to host getting treated: MOI-dependent

$$\begin{cases} BW4 = (1 + r_{0,U}) d_0 PW_{0,U} \\ BW5 = (1 + r_{1,U}) d_1 PW_{1,U} \\ BW6 = (1 + r_{2,U}) d_2 \frac{\omega}{n_{strains}} PW_{2,U} \end{cases} \tag{38}$$

Parasite Survival of Drug Treatment

$$\begin{cases} BW7 = \frac{PW_{0,D}}{\tau} \\ BW8 = \frac{PW_{1,D}}{\tau} \\ BW9 = \frac{PW_{2,D}}{\tau} \end{cases} \tag{39}$$

Transition due to Host Gain of Immunity

$$\begin{cases} BW10 = B_U(1 - \frac{r_{0,U}}{K})\rho_1(1-\eta_0) + \rho_1(1+r_{0,U})\mu_{PW_U} PW_{0,U} \\ BW11 = B_D(1 - \frac{r_{0,D}}{K})\rho_1(1-\eta_0) + \rho_1(1+r_{0,D})\mu_{PR_D} PW_{0,D} \\ BW12 = B_U(1 - \frac{r_{1,U}}{K})\rho_2(1-\eta_1) + \rho_2(1+r_{1,U})\mu_{PW_U} PW_{1,U} \\ BW13 = B_D(1 - \frac{r_{1,D}}{K})\rho_2(1-\eta_1) + \rho_2(1+r_{1,D})\mu_{PR_D} PW_{1,D} \end{cases} \tag{40}$$

Transition due to Host Loss of Immunity

$$\begin{cases} BW14 = (H_{1,U} h_{1,U} \frac{\exp(-\frac{h_{1,U}}{\Lambda})}{1-\exp(-\frac{h_{1,U}}{\Lambda})}) PW_{1,U} \\ BW15 = (H_{1,D} h_{1,D} \frac{\exp(-\frac{h_{1,D}}{\Lambda})}{1-\exp(-\frac{h_{1,D}}{\Lambda})}) PW_{1,D} \\ BW16 = (H_{2,U} h_{2,U} \frac{\exp(-\frac{h_{2,U}}{\Lambda})}{1-\exp(-\frac{h_{2,U}}{\Lambda})}) PW_{2,U} \\ BW17 = (H_{2,D} h_{2,D} \frac{\exp(-\frac{h_{2,D}}{\Lambda})}{1-\exp(-\frac{h_{2,D}}{\Lambda})}) PW_{2,D} \end{cases} \tag{41}$$

Parasites Removed due to Malarial Death

$$\begin{cases} BW18 = (1+r_{0,U})\mu_{PW_U}\mu_{0,U} PW_{0,U} \\ BW19 = (1+r_{0,D})\mu_{PR_D}\mu_{0,D} PW_{0,D} \end{cases} \tag{42}$$

Parasite Death due to Immunity or Drug Clearance in Different Host Environments

$$\begin{cases} BW20 = \mu_{PW_U} PW_{0,U} \\ BW21 = \mu_{PW_D} PW_{0,D} \\ BW22 = \mu_{PW_U} PW_{1,U} \\ BW23 = \mu_{PW_D} PW_{1,D} \\ BW24 = \mu_{PW_U} PW_{2,U} \\ BW25 = \mu_{PW_D} PW_{2,D} \end{cases} \tag{43}$$

Parasite Death due to Natural Host Death

$$\begin{cases} BW26 = \alpha PW_{0,U} \\ BW27 = \alpha PW_{0,D} \\ BW28 = \alpha PW_{1,U} \\ BW29 = \alpha PW_{1,D} \\ BW30 = \alpha PW_{2,U} \\ BW31 = \alpha PW_{2,D} \end{cases} \tag{44}$$

These rates can be thought of as accounting separately for new infections versus concurrent infections. The terms $(1+r_{i,j})$ are to account for the MOI-dependence explained and derived in the main text.

The ODEs for sensitive (wild-type) strains in the parasite model are as follows. (Note that hosts in G_2 can still be infected by local strains in the model, even if they do not experience symptoms.):

$$
\begin{cases}
\frac{dPR_{0,U}}{dt} = (BW1) + (BW7) + (BW14) - (BW4) - (BW10) - (BW18) - (BW20) - (BW26) \\
\frac{dPR_{0,D}}{dt} = (BW4) + (BW15) - (BW7) - (BW11) - (BW19) - (BW21) - (BW27) \\
\frac{dPR_{1,U}}{dt} = (BW2) + (BW8) + (BW10) + (BW16) - (BW5) - (BW12) - (BW14) - (BW22) - (BW28) \\
\frac{dPR_{1,D}}{dt} = (BW5) + (BW11) + (BW17) - (BW8) - (BW13) - (BW15) - (BW23) - (BW29) \\
\frac{dPR_{2,U}}{dt} = (BW3) + (BW9) + (BW12) - (BW6) - (BW16) - (BW24) - (BW30) \\
\frac{dPR_{2,D}}{dt} = (BW6) + (BW13) - (BW9) - (BW17) - (BW25) - (BW31)
\end{cases}
\tag{45}
$$

A similar set of rates is used for the formulation of the ODEs for the resistant parasite classes:

Infection Via Vector

$$
\begin{cases}
BR1 = B_{PR} H_{0,U} \eta_0 (1 - \frac{r_{0,U}}{K}) \\
BR2 = B_{PR} H_{1,U} \eta_1 (1 - \frac{r_{1,U}}{K}) \\
BR3 = B_{PR} H_{2,U} \eta_2 (1 - \frac{r_{2,U}}{K}) \\
BR4 = B_{PR} H_{0,D} \eta_0 (1 - \frac{r_{0,D}}{K}) \\
BR5 = B_{PR} H_{1,D} \eta_1 (1 - \frac{r_{1,D}}{K}) \\
BR6 = B_{PR} H_{2,D} \eta_2 (1 - \frac{r_{2,D}}{K})
\end{cases}
\tag{46}
$$

Transition due to Treatment

$$
\begin{cases}
BR7 = (1 + r_{0,U}) d_0 PR_{0,U} \\
BR8 = (1 + r_{1,U}) d_1 PR_{1,U} \\
BR9 = (1 + r_{2,U}) d_2 \frac{\omega}{n_{strains}} PR_{2,U}
\end{cases}
\tag{47}
$$

Loss of Drug Effectiveness

$$
\begin{cases}
BR10 = \frac{PR_{0,D}}{\tau} \\
BR11 = \frac{PR_{1,D}}{\tau} \\
BR12 = \frac{PR_{2,D}}{\tau}
\end{cases}
\tag{48}
$$

Transition due to Host Gain of Immunity

$$
\begin{cases}
BR13 = B_U (1 - \frac{r_{0,U}}{K}) \rho_1 (1 - \eta_0) + \rho_1 (1 + r_{0,U}) \mu_{PW_U} PR_{0,U} \\
BR14 = B_D (1 - \frac{r_{0,D}}{K}) \rho_1 (1 - \eta_0) + \rho_1 (1 + r_{0,D}) \mu_{PR_D} PR_{0,D} \\
BR15 = B_U (1 - \frac{r_{1,U}}{K}) \rho_2 (1 - \eta_1) + \rho_2 (1 + r_{1,U}) \mu_{PW_U} PR_{1,U} \\
BR16 = B_D (1 - \frac{r_{1,D}}{K}) \rho_2 (1 - \eta_1) + \rho_2 (1 + r_{1,D}) \mu_{PR_D} PR_{1,D}
\end{cases}
\tag{49}
$$

Transition due to Host Loss of Immunity

$$
\begin{cases}
BR17 = (H_{1,U} h_{1,U} \frac{\exp(-\frac{h_{1,U}}{\Lambda})}{1 - \exp(-\frac{h_{1,U}}{\Lambda})}) PR_{1,U} \\
BR18 = (H_{1,D} h_{1,D} \frac{\exp(-\frac{h_{1,D}}{\Lambda})}{1 - \exp(-\frac{h_{1,D}}{\Lambda})}) PR_{1,D} \\
BR19 = (H_{2,U} h_{2,U} \frac{\exp(-\frac{h_{2,U}}{\Lambda})}{1 - \exp(-\frac{h_{2,U}}{\Lambda})}) PR_{2,U} \\
BR20 = (H_{2,D} h_{2,D} \frac{\exp(-\frac{h_{2,D}}{\Lambda})}{1 - \exp(-\frac{h_{2,D}}{\Lambda})}) PR_{2,D}
\end{cases}
\tag{50}
$$

Transition due to Malarial Death

$$\begin{cases} BR21 = (1 + r_{0,U})\mu_{PW_U}\mu_{0,U}PR_{0,U} \\ BR22 = (1 + r_{0,D})\mu_{PR_D}\mu_{0,D}PR_{0,D} \end{cases} \tag{51}$$

Parasite Death in Different Host Environments

$$\begin{cases} BR23 = \mu_{PR_U}PR_{0,U} \\ BR24 = \mu_{PR_D}PR_{0,D} \\ BR25 = \mu_{PR_U}PR_{1,U} \\ BR26 = \mu_{PR_D}PR_{1,D} \\ BR27 = \mu_{PR_U}PR_{2,U} \\ BR28 = \mu_{PR_D}PR_{2,D} \end{cases} \tag{52}$$

Transition due to Natural Host Death

$$\begin{cases} BR29 = \alpha PR_{0,U} \\ BR30 = \alpha PR_{0,D} \\ BR31 = \alpha PR_{1,U} \\ BR32 = \alpha PR_{1,D} \\ BR33 = \alpha PR_{2,U} \\ BR34 = \alpha PR_{2,D} \end{cases} \tag{53}$$

The corresponding set of ODEs for resistant parasite populations is therefore

$$\begin{cases} \frac{dPR_{0,U}}{dt} = (BR1) + (BR10) + (BR17) - (BR7) - (BR13) - (BR21) - (BR23) - (BR29) \\ \frac{dPR_{0,D}}{dt} = (BR4) + (BR7) + (BR18) - (BR10) - (BR14) - (BR22) - (BR24) - (BR30) \\ \frac{dPR_{1,U}}{dt} = (BR2) + (BR11) + (BR13) + (BR19) - (BR8) - (BR15) - (BR17) - (BR25) - (BR31) \\ \frac{dPR_{1,D}}{dt} = (BR5) + (BR8) + (BR14) + (BR20) - (BR11) - (BR16) - (BR18) - (BR26) - (BR32) \\ \frac{dPR_{2,U}}{dt} = (BR3) + (BR12) + (BR15) - (BR9) - (BR19) - (BR27) - (BR33) \\ \frac{dPR_{2,D}}{dt} = (BR6) + (BR9) + (BR16) - (BR12) - (BR20) - (BR28) - (BR34) \end{cases} \tag{54}$$

It is assumed that the death rate of sensitive parasites in drug treated hosts μ_{PW_D} is much larger than either μ_{PW_U} or μ_{PR_U}, which are considered to be equal under the presumption that there is no fitness cost incurred on clearance rate in resistant parasites. In a situation where only one type of drug is being used in treatment, μ_{PR_D} is again equal or less than μ_{PW_U} and μ_{PR_U}, but under a policy change or other use of a drug with different loci conferring resistance, μ_{PR_D} can be defined as the harmonic mean of two rates,

$$\mu_{P_{R,D}} = 1/(Q/(\mu_{P_{R,U}}) + (1 - Q)/(\mu_{P_{W,D}})) \tag{55}$$

where Q is the proportion of drug treatments using the drug to which resistance is being investigated.

Immune Memory Submodel

The immune memory of the system is tracked as the total number of infections (TI) experienced by the hosts in G_0,$G-1$, and G_2 classes via 3 ODEs. The general approach to

writing the ODEs for these variables is to add the rate at which generalized immunity is gained, accounting for the movements of hosts between different G classes. Furthermore, it is not necessary to track the immune memory to resistant and sensitive parasites separately because the resistance status does not influence the gaining of specific or generalized immunity. The rates used in the ODEs for the immune memory classes are the following:

Increase of Cleared Infections

$$\begin{cases} C1 = H_{0,U}(B_U(1-\frac{r_{0,U}}{K})(1-\eta_0)+r_{0,U}\mu_{PW_U})+H_{0,D}(B_D(1-\frac{r_{0,D}}{K})(1-\eta_0)+r_{0,D}\mu_{PR_D}) \\ C2 = H_{1,U}(B_U(1-\frac{r_{1,U}}{K})(1-\eta_1)+r_{1,U}\mu_{PW_U})+H_{1,D}(B_D(1-\frac{r_{1,D}}{K})(1-\eta_1)+r_{1,D}\mu_{PR_D}) \\ C3 = H_{2,U}(B_U(1-\frac{r_{2,U}}{K})(1-\eta_2)+r_{2,U}\mu_{PW_U})+H_{2,D}(B_D(1-\frac{r_{2,D}}{K})(1-\eta_2)+r_{2,D}\mu_{PR_D}) \end{cases} \tag{56}$$

Loss of Infections Counts due to Immunity Loss and Host Death

$$\begin{cases} C4 = (\Lambda+\alpha)TI_0 \\ C5 = (\Lambda+\alpha)TI_1 \\ C6 = (\Lambda+\alpha)TI_2 \end{cases} \tag{57}$$

Immunity Carried by Hosts Moved from lower G to higher G

$$\begin{cases} C7 = (H_{0,U}(B_U(1-\frac{r_{0,U}}{K})\rho_1(1-\eta_0)+\rho_1 r_{0,U}\mu_{PW_U})+H_{0,D}(B_D(1-\frac{r_{0,D}}{K})\rho_1(1-\eta_0)+\rho_1 r_{0,D}\mu_{PR_D}))v_0 \\ C8 = (H_{1,U}(B_U(1-\frac{r_{1,U}}{K})\rho_2(1-\eta_1)+\rho_2 r_{1,U}\mu_{PW_U})+H_{1,D}(B_D(1-\frac{r_{1,D}}{K})\rho_2(1-\eta_1)+\rho_2 r_{1,D}\mu_{PR_D}))v_1 \end{cases} \tag{58}$$

Immunity Carried by Hosts Moved from higher G to lower G

$$\begin{cases} C9 = (H_{1_U}(h_{1,U}\frac{\exp(-\frac{h_{1,U}}{\Lambda})}{1-\exp(-\frac{h_{1,U}}{\Lambda})})+H_{1_D}(h_{1,D}\frac{\exp(-\frac{h_{1,D}}{\Lambda})}{1-\exp(-\frac{h_{1,D}}{\Lambda})}))v_1 \\ C10 = (H_{2,U}(h_{2,U}\frac{\exp(-\frac{h_{2,U}}{\Lambda})}{1-\exp(-\frac{h_{2,U}}{\Lambda})})+H_{2,D}(h_{2,D}\frac{\exp(-\frac{h_{2,D}}{\Lambda})}{1-\exp(-\frac{h_{2,D}}{\Lambda})}))v_2 \end{cases} \tag{59}$$

The three ODEs describing the immune memory of the hosts are

$$\begin{cases} \frac{dTI_0}{dt} = (C1)+(C9)-(C4)-(C7) \\ \frac{dTI_1}{dt} = (C2)+(C7)+(C10)-(C5)-(C9)-(C8) \\ \frac{dTI_2}{dt} = (C3)+(C8)-(C6)-(C10) \end{cases} \tag{60}$$

Solving these ODEs gives the number of cumulative infections experienced by members of that host class at time t. The average number of such infections experienced by a member of the host class is v_i at time t such that

$$\begin{cases} v_0 = \frac{TI_0}{H_{0_U}+H_{0_D}} \\ v_1 = \frac{TI_1}{H_{1_U}+H_{1_D}} \\ v_2 = \frac{TI_2}{H_{2_U}+H_{2_D}} \end{cases} \tag{61}$$

These v values can then be used in equation (1) to determine the infectivities of each host class (the η_i values).

Final Implementation

A final addition to the model was to add the potential for seasonal variation in contact rate b. b was set equal to a continuous, differentiable function of time:

$$b(t) = -b_{avg} L cos(\kappa sin(\frac{t+p_s}{a}) - \frac{t+p_s}{a}) + b_{avg} \quad (62)$$

where b_{avg} is the average yearly contact rate; L, on an interval of 0 to 1, is the amplitude of seasonal fluctuations relative to b_{avg}; κ, which is only biologically reasonable on the interval -1 to 1, controls the relative length of the dry season; p_s is the phase shift, and a is the period of oscillations. It should be noted that this approach to describing seasonal fluctuations is limited in how long of a dry season it can describe (because $\kappa > 1$ leads to a function with no biological implications).

A generalized immunity-only model was then specified as a counterpoint to the model incorporating specific immunity; in this model, the values of η_i were decoupled from the accumulated infections, and were set equal to a fixed value: $\eta_0 = 0.927, \eta_1 = 0.685, \eta_2 = 0.317$. These values were the mean infectivities of the immunity classes over the range of parameter space at equilibrium from our full model. This procedure implies that there is no limit from strain-specific immune memory on infectivity.

The entire system of ODEs was solved numerically for the range of parameter values listed in ***Appendix 1***-Table 1 using the package deSolve (***Soetaert et al., 2010***) in R (***R Core Team, 2023***), and the results were plotted and analyzed using packages tidyverse (***Wickham et al., 2019***) and ggplot2 (***Wickham, 2016***), also in R.

Appendix 1—table 1. Epidemiological parameters used for numerically solving ODEs. All rates are measured per day; time is measured in days.

Symbol	Type	Description	Values
b_{avg}	rate	average yearly contact rate	[0.0126-10]
$n_{strains}$	number	local strain diversity	[6-447]
τ	time	period of drug effectiveness	20
ω	probability	chance of symptoms for G_2	0.01
ρ_1	probability	transition probability to G_1	0.5
ρ_2	probability	transition probability to G_2	0.05
s_{single}	number	clonal cost of resistance	[0.1-0.3]
s_{mixed}	number	mixed-infection cost of resistance	[0.3-0.9]
K	number	carrying capacity	10
μ_{PW_U}	rate	WU clearance rate	1/150
μ_{PW_D}	rate	WD clearance rate	0.99
μ_{PR_U}	rate	RU clearance rate	1/150
μ_{PR_D}	rate	RD clearance rate	1/150
d_i	rate	daily treatment rate of symptomatic	[0.05,0.2]
L	scale factor	amplitude of seasonal fluctuations	0.95
κ	scale factor	relative length of dry season	1
p_s	number	phase shift of seasonal fluctuations	0
a	time	period of seasonal fluctuations	365/(2π)
Q	proportion	proportion of drug treatments using focus drug	[0-1] (see ***Figure 6*** caption)
δ	rate	daily constant host birth rate	1 host
$\mu_{0,U}$	rate	daily death rate of 0U hosts due to malaria	1/1500
$\mu_{0,D}$	rate	daily death rate of 0D hosts due to malaria	1/1500
α	rate	death rate in absence of malaria	1/(50*365)
Λ	rate	rate of immunity loss	0.001

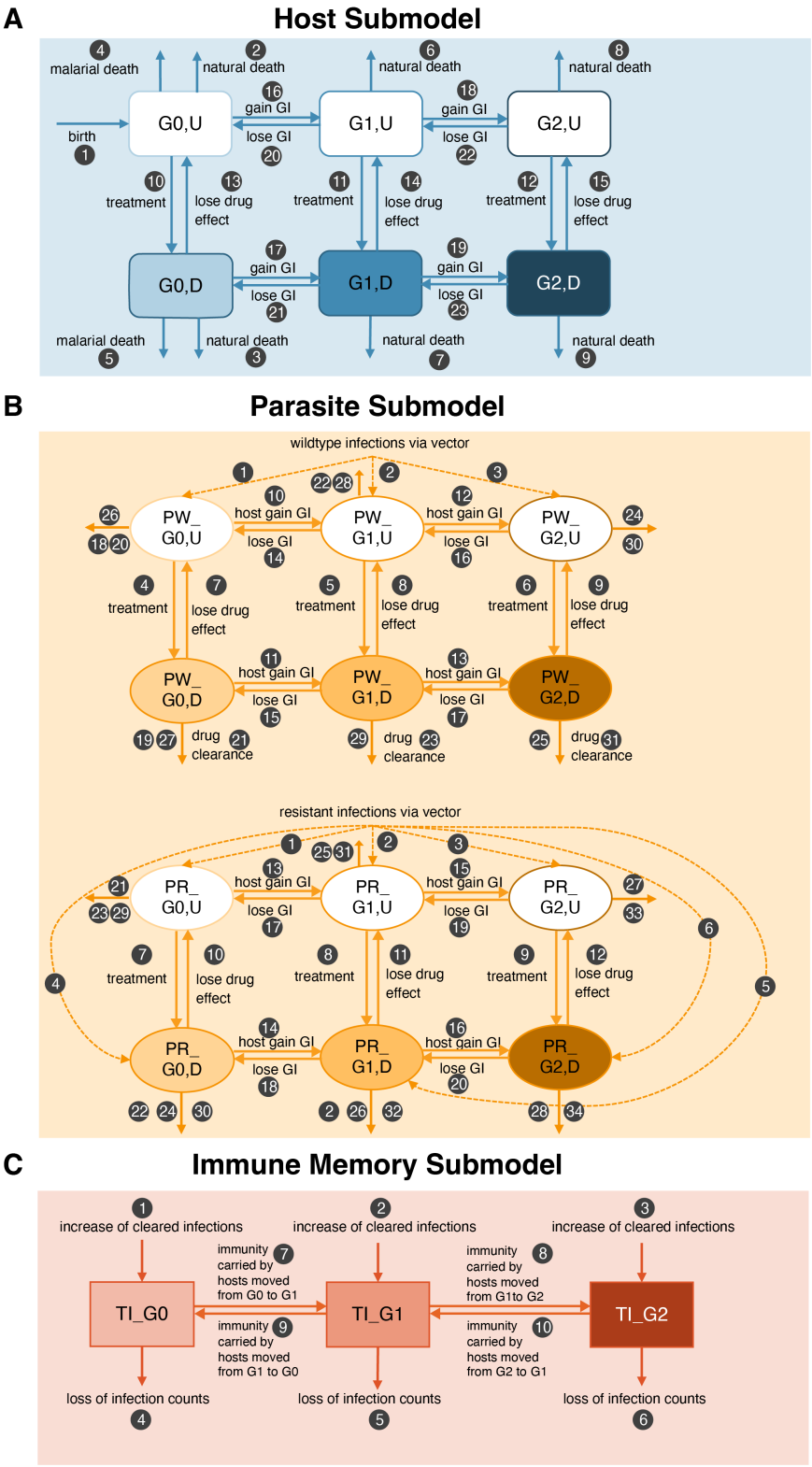

Figure 1—figure supplement 1. Compartment model of drug resistance evolution. **(A)** The number of hosts and movements are tracked in different generalized immunity classes (G), together with their drug treatment states (treated, D; untreated, U); **(B)** wild-type (PW) and resistant parasite (PR) population sizes are tracked in different host immunity classes; **(C)** Changes in total immunity (TI, total number of cleared infections) per G class are followed. See ***Appendix 1*** for a detailed explanation of the ODE system.

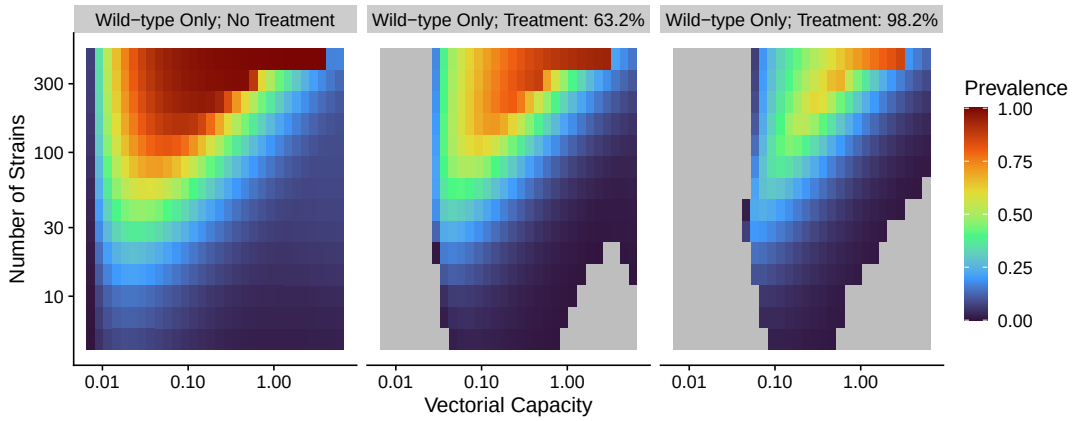

Figure 2—figure supplement 1. Prevalence given the combination of vectorial capacity and the number of strains from no treatment to high treatment rate for wild-type-only infections. Grey areas indicate that transmission is eliminated.

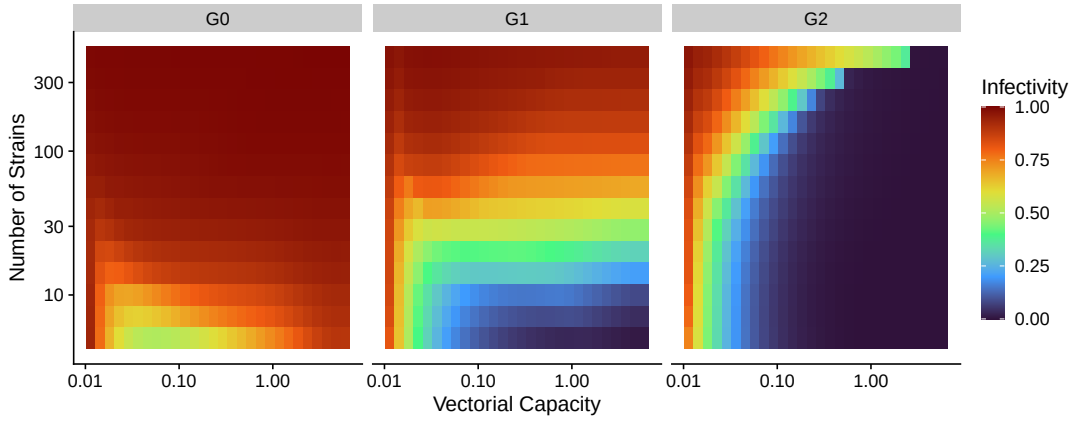

Figure 2—figure supplement 2. Infectivity of a new infection as a function of the number of strains and mean immunity. (Total immunity divided by the number of hosts per G class) (see Eq. 1. s_{single}: 0.1; s_{mixed}: 0.9.

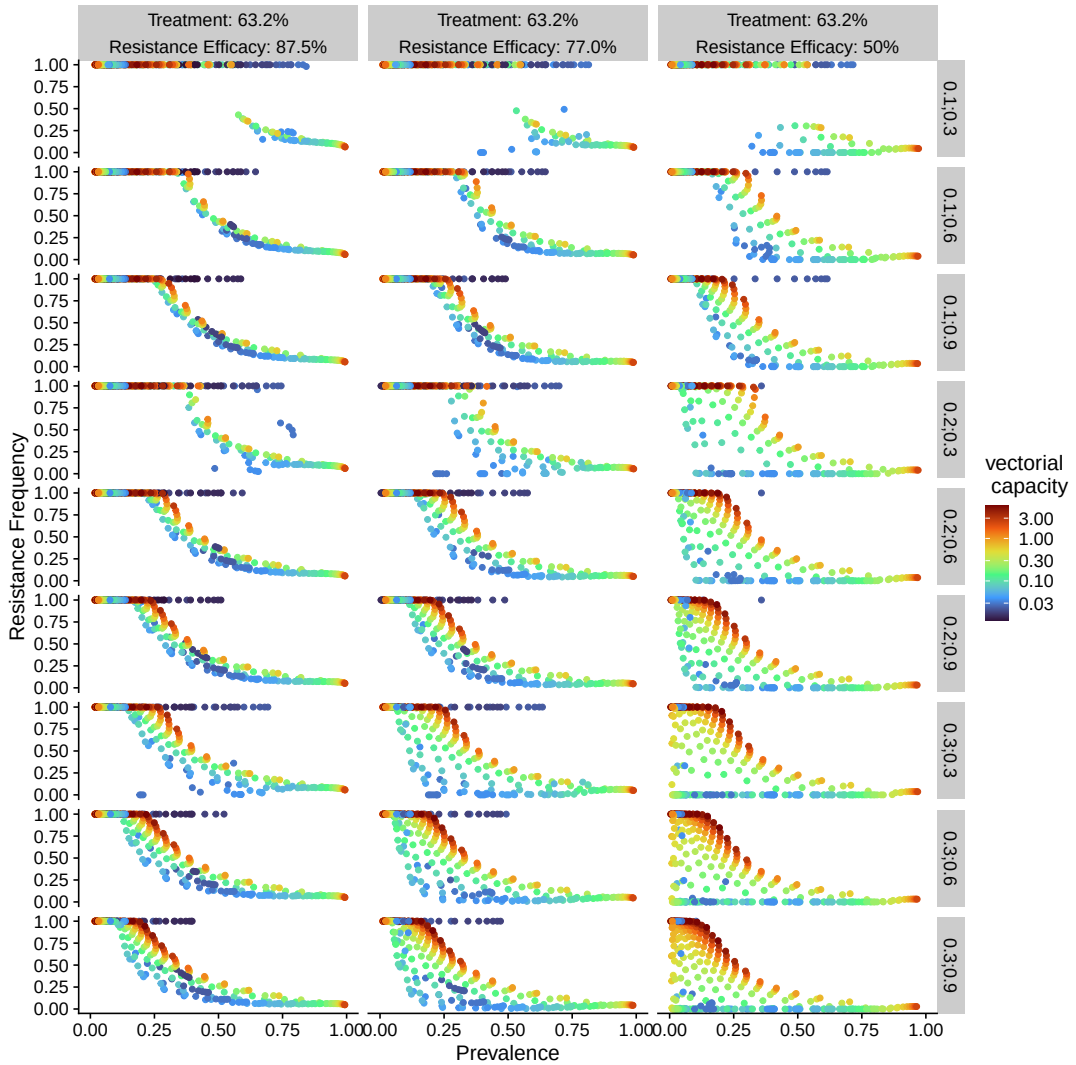

Figure 2—figure supplement 3. Relationship between parasite prevalence and resistance frequency under full treatment (daily treatment rate $d1 = 0.2$). Each subgraph represents the combination of resistance fitness costs in hosts with resistant strains alone (s_{single}) and mixed-genotype infections of resistant and wild-type strains (s_{mixed}), as well as the efficacy of resistance ($mu_{P_{RD}}$). Color indicates vectorial capacity.

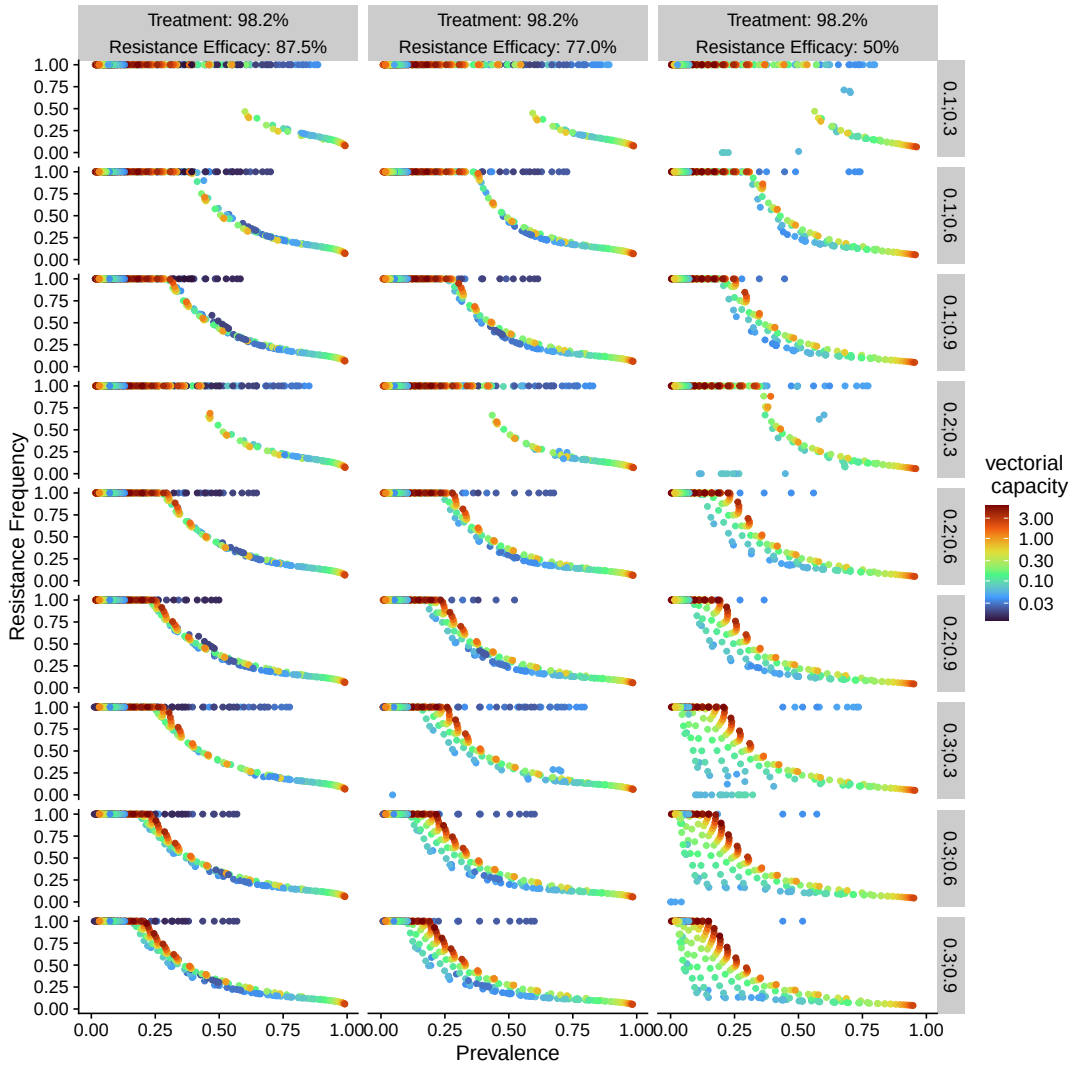

Figure 2—figure supplement 4. Relationship between parasite prevalence and resistance frequency under partial treatment (daily treatment rate $d1 = 0.2$). Each subgraph represents the combination of resistance fitness costs in hosts with resistant strains alone (s_{single}) or mixed-genotype infections of resistant and wild-type strains (s_{mixed}). Color indicates vectorial capacity, as well as the efficacy of resistance ($mu_{P_{RD}}$).

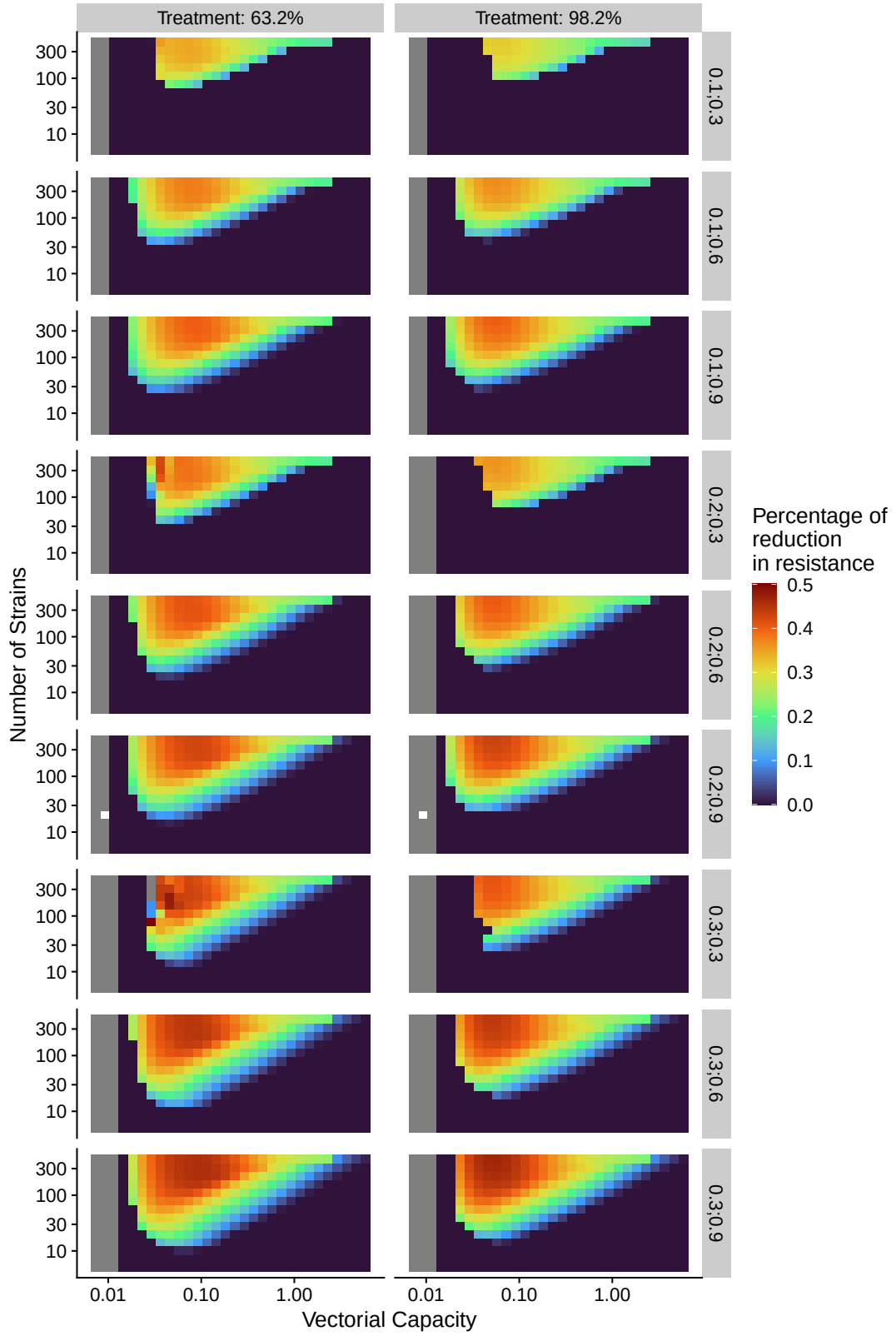

Figure 6—figure supplement 1. Percentage of reduction in resistance after one year of policy change in drug treatment as a function of vectorial capacity and the number of strains under different combinations of resistance costs (s_{single};s_{mixed}).

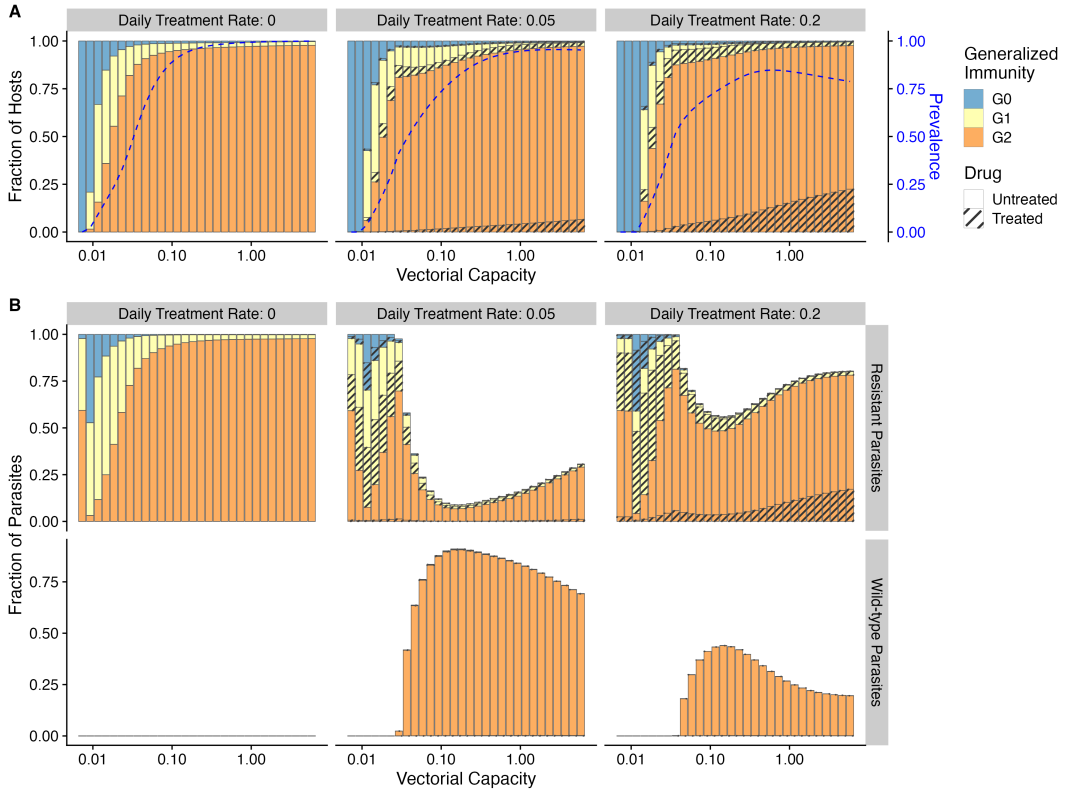

Figure 8—figure supplement 1. Relationship between host immunity, drug treatment, and resistance evolution for the generalized-immunity-only model. Note that in the generalized-immunity-only model, there is no strain diversity. The only parameter that determines transmission intensity is vectorial capacity. In general, prevalence (blue dotted line) increases as vectorial capacity increases despite hosts increasingly concentrating in G_2 class **(A)**. The fraction of resistant parasites decreases initially with increasing vectorial capacity, but rises again as high transmission results in a higher proportion of G_2 hosts in the drug-treated class **(B)**.